- 1 Salinity pulses interact with seasonal dry-down to increase ecosystem carbon loss in marshes of
- 2 the Florida Everglades

3

- 4 Authors: Benjamin J. Wilson<sup>1</sup>, Shelby Servais<sup>1</sup>, Viviana Mazzei<sup>1</sup>, John S. Kominoski<sup>1</sup>, Minjie
- 5 Hu<sup>2</sup>, Stephen E. Davis<sup>3</sup>, Evelyn Gaiser<sup>1</sup>, Fred Sklar<sup>4</sup>, Laura Bauman<sup>1</sup>, Stephen Kelly<sup>4</sup>,
- 6 Christopher Madden<sup>4</sup>, Jennifer Richards<sup>1</sup>, David Rudnick<sup>5</sup>, Joseph Stachelek<sup>4,6</sup>, and Tiffany G.
- 7 Troxler<sup>1,7</sup>

8

- 9 <sup>1</sup>Florida International University, Dept. of Biological Sciences and Southeast Environmental
- 10 Research Center, Miami, FL 33199
- <sup>2</sup>College of the Environment and Ecology, Xiamen University, Xiamen 361002, China
- <sup>3</sup>Everglades Foundation, Palmetto Bay, FL 33157
- <sup>4</sup>South Florida Water Management District, West Palm Beach, FL 33406
- <sup>5</sup>Everglades National Park, Homestead, FL 33034
- 15 <sup>6</sup>Michigan State University, East Lansing, MI 48824
- <sup>7</sup>Sea Level Solutions Center, Florida International University, Miami, FL 33199

17

#### Abstract

18

19

20

21

22

23

24

25

26

27

28

29

30

31

32

33

34

35

36

37

38

39

40

Coastal wetlands are globally important sinks of organic carbon (C). However, to what extent wetland C cycling will be affected by accelerated sea-level rise (SLR) and saltwater intrusion is unknown, especially in coastal peat marshes where water flow is highly managed. Our objective was to determine how the ecosystem C balance in coastal peat marshes is influenced by elevated salinity. For two years, we made monthly in situ manipulations of elevated salinity in freshwater (FW) and brackish water (BW) sites within Everglades National Park, FL, USA. Salinity pulses interacted with marsh-specific variability in seasonal hydroperiods whereby effects of elevated pulsed salinity on gross ecosystem productivity (GEP), ecosystem respiration (ER), and net ecosystem productivity (NEP) were dependent on marsh inundation level. We found little effect of elevated salinity on C cycling when both marsh sites were inundated, but when water levels receded below the soil surface, the BW marsh shifted from a C sink to a C source. During these exposed periods, we observed an approximately 3-fold increase in CO<sub>2</sub> efflux from the marsh as a result of elevated salinity. Initially, elevated salinity pulses did not affect Cladium jamaicense biomass, but aboveground biomass began to be significantly lower in the saltwater amended plots after two years of exposure at the BW site. We found a 65% (FW) and 72% (BW) reduction in live root biomass in the soil after two years of exposure to elevated salinity pulses. Regardless of salinity treatment, the FW site was C neutral while the BW site was a strong C source (-334 to -454 g C m<sup>-2</sup> y<sup>-1</sup>), particularly during dry-down events. A loss of live roots coupled with annual net CO<sub>2</sub> losses as marshes transition from FW to BW likely contribute to the collapse of peat soils observed in the coastal Everglades. As SLR increases the rate of saltwater intrusion into coastal wetlands globally, understanding how water management influences C gains and losses from these systems is crucial. Under current Everglades' water management,

drought lengthens marsh dry-down periods, which, coupled with saltwater intrusion, accelerates

CO<sub>2</sub> loss from the marsh.

Keywords: sea level rise, saltwater intrusion, sawgrass, biogeochemistry, peat collapse, drought,
 wetlands, blue carbon

# **Introduction**

Coastal wetlands are some of the most productive ecosystems in the world and are known for their capacity to store disproportionately large amounts of carbon (C) in their soils despite their relatively small global coverage (Chmura et al. 2003, Duarte et al. 2005, McLeod et al. 2011). Yet storage of wetland C is highly vulnerable to changing environmental conditions, such as salinity and hydrology. With sea levels rising at ~3 mm y<sup>1</sup> (Zhang et al. 2011), coastal freshwater and intertidal wetlands are being exposed to increased duration and spatial extent of inundation and potentially higher-salinity water (Herbert et al. 2015).

The Florida Everglades, USA, is one of the largest wetland ecosystems in the world, an International Biosphere Reserve, a UNESCO World Heritage Site, and a Ramsar Wetland of International Importance. The Everglades contains vast amounts of C in its peat soils (Davis et al. 1994, Jerath et al. 2016); however, the Everglades contains only ~24% of its original peat volume because of anthropogenic modification (Hohner and Dreschel 2015), and climate change pressures keep this wetland in a state of fluctuation that may potentially alter its C storage capacity. In the early part of the 20<sup>th</sup> century, the construction of canals and levees diverted the flow of water away from the southern coastal Everglades, reducing water tables by as much as 2.7 m and resulting in the loss of half the ecosystem (McVoy et al. 2011; Sklar et al. *in press*).

64

65

66

67

68

69

70

71

72

73

74

75

76

77

78

79

80

81

82

83

84

85

86

The reduction in freshwater flow into the southern Everglades has reduced the freshwater head, resulting in faster-than-expected saltwater intrusion into the Biscayne Aquifer, which lies underneath the Everglades (Klein and Waller 1985, Saha et al. 2011). In addition to greater saltwater intrusion, less water flowing into the Everglades means more periods of "dry-down," when water recedes below the soil surface (Sklar et al. 2000). Extended dry-down periods can enhance C loss from the wetland through greater soil oxidation and microbial metabolism (Wright and Reddy 2001, Reddy and DeLaune 2008). As climate change is expected to change rainfall patterns in southern Florida (Allan and Soden 2008, Li et al. 2012), greater magnitude and longer dry-down events are possible (Obeysekera et al. 2015), which can further exacerbate saltwater intrusion and affect ecosystem C dynamics (see below). Steps have been taken to increase freshwater delivery to the coastal Everglades: under the Comprehensive Everglades Restoration Plan (CERP) authorized in 2000, a series of 60+ projects were proposed to restore the flow of water back to the southern Everglades (Sklar et al. 2005). However, as of 2017, the most critical central decompartmentalization projects still await Federal funding, and flows to the southern Everglades are still not up to CERP target levels (National Academies of Sciences 2016). The continued intrusion of saltwater into the coastal Everglades has, in some areas, caused drastic changes to the landscape, such as "peat collapse" and the conversion of coastal marshes to open water ponds (Wanless and Vlaswinkel 2005). In the low-lying and gently sloping coastal Everglades, the effects of saltwater intrusion may be amplified by having a lower freshwater head, due to current water management strategies, and by storm surges caused by tropical storms. Storm surges bring pulses of saltwater into nearshore brackish-to-freshwater marshes that can impact ecosystem structure, function, and, ultimately, persistence (Herbert et al. 2015). In historically freshwater marshes, pulses of

elevated salinity water can cause ions, such as ammonium (NH<sub>4</sub><sup>+</sup>), that are adsorbed onto cation exchange sites, to be displaced by ions found in seawater, such as Na<sup>+</sup>, Mg<sup>2+</sup>, and Ca<sup>2+</sup> (Seitzinger et al. 1991, Weston et al. 2010). The newly accessible NH<sub>4</sub><sup>+</sup> may be available for vascular plant uptake, especially in N-limited wetlands, but N uptake rates may slow as salt stress and sulfide (HS<sup>-</sup>) toxicity suppress plant growth (Spalding and Hester 2007, Cormier et al. 2013). Greater SO<sub>4</sub><sup>2-</sup> availability can increase microbial metabolism and the production of HS<sup>-</sup> (Lamers et al. 1998, Weston et al. 2011), but it can also lead to a decrease in methane (CH<sub>4</sub>) production as methanogens are outcompeted for substrates (Capone and Kiene 1988, Burdige 2006).

Saltwater intrusion can lead to changes in soil biogeochemical cycling that affects ecosystem C dynamics (Weston et al. 2011, Herbert et al. 2015). Many studies have documented changes in C cycling along coastal marsh salinity gradients, often with contrasting results as to whether increasing salinity enhances or depresses C storage (Neubauer 2013, Weston et al. 2014, Wilson et al. 2015, Herbert et al. 2018). While the effect on ecosystem C cycling of saltwater pulses into tidal marshes has been studied (e.g., Chambers et al. 2013, Neubauer 2013, Weston et al. 2014), the biogeochemical and ecosystem C responses of non-tidal, nearshore fresh- and brackish-water marshes to saltwater pulses is still not well known. Most research to date has focused on laboratory experiments (Weston et al. 2006, Chambers et al. 2011, Weston et al. 2011), mesocosm manipulations (Chambers et al. 2013, Wilson et al. 2018), or natural salinity gradients in the field (Craft et al. 2009, Giblin et al. 2010, Weston et al. 2014, Wilson et al. 2015, Whittle and Gallego-Sala 2016). Very few salinity manipulations have been conducted in the field (Neubauer 2013, Herbert et al. 2018), but since scale often matters to interpretation of results, in situ manipulations are desirable for deducing mechanisms of change inferred from

smaller-scale/benchtop experiments or larger-scale descriptive studies.

Our objective was to test ecosystem responses to pulses of elevated salinity in both freshwater and brackish water peat marshes in the coastal Everglades. We experimentally elevated *in situ* porewater salinity to twice-ambient levels using monthly pulsed deliveries to surface waters of brackish and freshwater marshes. We measured C fluxes (as CO<sub>2</sub> and CH<sub>4</sub>), above- and below-ground *Cladium jamaicense* (sawgrass) biomass and production, and porewater biogeochemical constituents to understand critical process changes in ecosystem function. We hypothesized that (1) prolonged exposure to pulsed salinity increases would alter belowground biogeochemical cycling and reduce net ecosystem productivity (NEP) in freshwater and brackish peat marshes; (2) the decline in NEP contributes to net soil C loss and less sawgrass fine root production; (3) C loss from the soil will be amplified during conditions of seasonal drydown and/or drought; and (4) the freshwater (FW) marsh will be more sensitive to saltwater intrusion than the brackish water (BW) marsh and would therefore have higher magnitude responses to the elevated salt treatment.

# Methods

# Study Sites and Experimental Design

This study was conducted in Everglades National Park, Florida, USA along the southeastern boundary of Shark River Slough, the largest drainage basin in the southern Everglades. The coastal Everglades range along a gradient from freshwater sawgrass ridges and sloughs to coastal mangrove forests. We chose two sites for our study: a brackish marsh that was already experiencing saltwater intrusion and a freshwater marsh that, to our knowledge, had not experienced elevated salinity. The brackish marsh (25°13'13.17" N, 80°50'36.96" W) was

dominated by *Cladium jamaicense* (sawgrass) sparsely interspersed with *Conocarpus erectus* (buttonwood). The site had an elevation of -0.90 cm and was non-tidal and characterized by distinct wet-dry hydrologic regimes in which the site was flooded for ~8 months out of the year (mean since 2000, Everglades Depth Estimation Network (EDEN) at station NMP). The freshwater marsh (25°26'07.77" N, 80°46'51.50" W) had an elevation of 0.27 cm and was codominated by sawgrass and *Eleocharis cellulosa* (spikerush) but also contained other freshwater marsh plants such as *Crinum americanum* (swamp lily), *Bacopa caroliniana* (waterhyssop), and *Panicum hemitomon* (maidencane). The hydrologic regime at the site was characterized as long-hydroperiod, flooded nearly year-round (~11 months, mean since 2000, EDEN at station NP62) during a typical season. The soil properties of each site are given in Table 1.

In September 2014, 16 plots were established at each site along an 80-m long constructed boardwalk (Fig. 1). In twelve plots, we installed 1.4-m diameter, 0.4-m tall clear, cylindrical, polycarbonate chambers by inserting them 30-cm into the soil. We designated 4 additional plots as "no-chamber" controls, and these had no chamber installed around them. Each chamber had a movable collar with a series of 10-cm diameter holes that could be closed during application of dosing water but were open to natural flow at all other times. Six ambient-water addition ("+AMB") plots were established upstream in the natural flow, while 6 treatment (+saltwater, "+SALT") plots were established downstream to avoid salt contamination into the +AMB and "no-chamber" control plots. The 4 "no-chamber" controls, which were interspersed within the +AMB plots (Fig. 1), did not receive any water additions and were used only for C flux and redox potential measurements (*see below*). A 3-m "buffer zone" was established to avoid contamination between salt-dosing and control plots.

# In Situ Saltwater Additions

156

157

158

159

160

161

162

163

164

165

166

167

168

169

170

171

172

173

174

175

176

177

Experimental water additions began in October 2014 and were conducted monthly for 2 vears (see Stachelek et al. (2018) for detailed methods). The volume and salinity of brine solution mixed to deliver our dose varied for each dosing month in order to reach porewater concentration targets. The volume and salinity of the brine solution was calculated based on both water height from soil surface and surface water salinity so that we could reach the target of twice ambient porewater salinity, 2-5 ppt at the FW site and 20 ppt at the BW site. Our brine solution during dosing ranged from 30.7-65.0 ppt at the FW site and 26.8-68.0 ppt at the BW site (Stachelek et al. 2018). The dosing solution was prepared using source water obtained at each study site (when the marsh was wet) or from a nearby canal (when the marsh was dry) with similar nutrient concentrations found in freshwater wetlands of the Everglades (C-111; 25°17'31.74" N, 80°27'21.59" W; Wilson et al. 2018); source water was combined with a commercially available sea salt mix (Instant Ocean ® (Atkinson and Bingman 1997)). An equal volume of site surface water or canal water was added to the +AMB plots each month to account for the addition of water in the absence of salinity. The movable collar on the chambers was used to close the chambers while dosing to ensure that the dosing water remained within the chamber. Doses were delivered from elevated boardwalks running alongside each chamber using a submersible bilge-style pump (Xylem Inc, USA). The outlet hose was fitted with a spreader device that split the large output stream into six smaller streams. This design was intended to maximize mixing with ambient site water while minimizing disturbance to sensitive benthic periphyton. Emergent plants were briefly sprayed with freshwater following dosing to avoid potential damage from direct salt application.

Chambers remained closed for 24 hours to allow the elevated-salinity water to penetrate into the porewater, then chambers were opened to prevent closure artifacts.

#### Soil and Water Chemistry

Porewater salinity and nutrient measurements were made from three sampling wells ("sippers") placed randomly inside each chamber to a depth of 15-cm. Porewater salinity was measured 24 and 120 hours after dosing. Two sippers were installed 0.5-m outside the edge of each chamber to monitor any potential leakage of saltwater outside of the treatment plots.

Samples for nutrient and carbon analyses were collected 24 h after dosing. From each sipper, a ~25-mL sample was extracted after purging the length of tubing, and temperature and salinity were measured immediately in the field (YSI Model 600 XL, Yellow Springs, OH). The porewater from each of the three wells was then combined into one sample per chamber (~75mL total), field-filtered (0.7 μm GF/F), transferred to new, single-use bottles, stored at 20°C, and analyzed within 21 d.

Surface water salinity was collected from each plot during wet periods by collecting 140-

Surface water salinity was collected from each plot during wet periods by collecting 140-mL of sample water and processing the same as porewater. Surface water temperature and salinity were measured immediately in the field (YSI). Soluble reactive phosphorus (SRP) and total dissolved P (TDP) were analyzed at the South Florida Water Management District Analytical Research Laboratory on an Alpkem Flow Solution Analyzer (OI Analytical, College Station, TX, USA) following Standard Method 4500-PF (SRP) and Solorzano and Sharp (1980, TDP). Ammonium (NH<sub>4</sub><sup>+</sup>), and dissolved inorganic N (DIN) were analyzed at the South Florida Water Management District Water Quality Laboratory on a Lachat Flow Injection Analyzer (Lachat Instruments, Loveland, CO, USA) following Standard Method 4500-NH3 H (NH<sub>4</sub><sup>+</sup>) or

Standard Method 4500-N C (DIN). Dissolved organic C (DOC) was analyzed using a Shimadzu TOC-L analyzer (Shimadzu Scientific Instruments, Columbia, MD, USA) following Standard Method 5310 B. Alkalinity and pH were determined using an automated titrator (Metrohm 855 Titrator, Herisau, Switzerland) following Standard Method 2320 B (Alkalinity) and a modification to Standard Method 4500 H<sup>+</sup> B (pH). Chloride (Cl<sup>-</sup>) and sulfate (SO<sub>4</sub><sup>2-</sup>) were measured using a Metrohm 881 Compact IC Pro System (Metrohm, Riverview, FL, USA) following Standard Method 4110 B. Sulfide (HS<sup>-</sup>) was measured using standard methods (McKee et al. 1988). Soil redox potential was measured using standard techniques (Faulkner et al. 1989); briefly, three platinum-tipped probes were inserted to 15-cm depth in each plot and allowed to equilibrate for 30 minutes before measurement. Soil bulk density was determined at the end of the experiment by taking one 2.4-cm diameter core per chamber down to 30-cm. Samples were dried at 60°C and weighed to calculate dry bulk density (g cm<sup>-3</sup>).

#### Species Richness, Culm Density, and Above- and Below-ground Biomass

Aboveground vegetation at each site was measured every other month using a non-destructive technique (Daoust and Childers 1998). Briefly, ten sawgrass plants per plot were tagged and turnover was determined from the change in the number of live and dead leaves. Within each plot during each sampling period, fifteen sawgrass plants were randomly chosen for leaf number, height of the longest leaf, and culm diameter measurements. Average aboveground sawgrass biomass was then calculated using previously-generated allometric equations (Childers et al. 2006). Sawgrass leaves were sampled yearly by collecting the youngest mature leaf from 3 randomly selected culms in each plot. These were dried and ground before analysis for C, nitrogen (N; Zimmermann and Keefe 1997), and phosphorus (P; Solorzano and Sharp 1980)

content. Macrophyte species richness was estimated by identifying and recording the genus and species of each plant taxon within each plot.

Live belowground root biomass was obtained by taking three 2.4-cm diameter soil cores from each plot at the end of year 2 (October 2016). Each core was taken to 30-cm depth, extruded, separated into 10-cm depths, and stored at 4°C until analysis (within 1 week). In the lab, the core segment was placed over a 1-mm sieve and washed with a constant stream of water. Live roots, those which floated when submerged in water, were separated from dead roots and peat, dried at 60°C, and weighed.

## Ecosystem Carbon Flux

Within each plot, one 0.5 x 0.5 m polycarbonate collar was permanently installed 10-cm into the soil and extended 5-cm above the soil surface for ecosystem C flux measurements. Each collar had eight 2.5-cm diameter holes at the soil surface level to allow for natural flow of water when measurements were not occurring. Plot-scale CO<sub>2</sub> exchange was measured monthly using a transparent static chamber (0.25 m<sup>2</sup> x 1.5 m; after Neubauer et al. 2000, Wilson et al. 2015). Prior to measurements being taken, each hole in the collar was plugged with a rubber stopper, the chamber was placed into a lip in the collar and sealed, and the system was allowed to equilibrate for 2 minutes. Measurements were then made for 3 minutes each in full light and in the dark, with the chamber lid removed in between each measurement to allow the chamber to return to atmospheric conditions (LI-COR 840, Lincoln, NE; Wilson et al. *in press*). All measurements made at each site were taken within ± 3 hours of solar noon and on the same day. Missing

when water levels were higher than the boardwalk (FW site, Dec 2015 – Apr 2016), limiting access to the plots.

Methane exchange measurements were conducted monthly from October 2014 – February 2016. After the dark CO<sub>2</sub> exchange measurement was conducted, the chamber was kept in the dark and resealed for 20 minutes. Air from the chamber was continually pumped through a closed loop with a sampling port attached. Gas samples were taken at 0, 10, and 20 minutes using a 60-mL syringe to withdraw 25-mL of air from the sampling port placed in line with the chamber. The sample was then injected into a 20-mL evacuated vial. Methane concentrations were determined using a gas chromatograph (Hewlett-Packard 5890, Palo Alto, CA, USA), and the change in concentration over time was used to calculate the flux.

Soil respiration was measured using one 10-cm diameter collar installed 5-cm into the soil surface within each plot at each site and were taken during dry-down. Soil CO<sub>2</sub> efflux was measured over one 1-day period in May 2015 at both sites when water receded below the soil surface; it was measured for 120 seconds using a portable infrared gas analyzer (LI-COR 8100, Lincoln, NE, USA). Soil CO<sub>2</sub> efflux was not measured during other dry months because of equipment failure.

## Statistical Analyses

The following analyses were performed in RStudio (V 1.1.383, RStudio, Inc.). The difference in biogeochemical variables (Cl<sup>-</sup>, SO<sub>4</sub><sup>2-</sup>, NH<sub>4</sub><sup>+</sup>, TDN, DOC, SRP, TDP, HS, alkalinity, and pH), gas flux (GEP, ER<sub>CO2</sub>, ER<sub>CH4</sub>, NEP, soil CO<sub>2</sub> efflux), culm density, and sawgrass biomass (above- and below-ground) among control, elevated salinity, and ambient water dosing experimental plots were evaluated using linear mixed-effects models (Package "nlme", Pinheiro

et al. 2017). Treatment and date were fixed factors, while plot was a random factor. Because hydrology highly influenced fluxes at the sites, analyses for gas fluxes were performed separately when each site was wet (water covering soil surface) and dry (water below soil surface). A two-way ANOVA was used to compare differences in plant nutrient concentrations across treatments and sites. All linear mixed models were assessed for temporal differences using the least squared means (LSMEANS), with date as a model effect (R package "Ismeans", Lenth 2017). All ANOVA analyses were sub-tested with Tukey's post-hoc test to see differences among treatments. Differences in total belowground biomass, soil CO2 efflux, and macrophyte species richness were determined using an independent t-test. Normality and homoscedasticity were tested by visually inspecting plotted residuals, and data were log-transformed to decrease heteroscedasticity when necessary. A piecewise regression with 200 iterations was used to determine change-points in ambient porewater salinity at the BW site using Sigmaplot 13.0 (Systat Software Inc., San Jose, CA). All analyses were tested with  $\alpha$ =0.10 because of the high within-site variability and because it was logistically unfeasible to increase replication power (Neubauer 2013). Therefore, type I errors (incorrectly rejecting the null hypothesis) are more likely than if a more conservative alpha value of 0.05 was used (Neubauer 2013).

285

286

284

269

270

271

272

273

274

275

276

277

278

279

280

281

282

283

# Results

287

288

289

290

291

#### Water Chemistry

Porewater salinity and chemistry at the FW and BW sites were measured 24 h after dosing. Porewater salinity in the +SALT plots at the FW site ranged from  $1.50 \pm 0.29$  to 4.56 ppt  $\pm 0.30$  (mean  $\pm$  SE; Fig. 2c) and was  $2.39 \pm 0.15$  ppt higher compared to ambient fresh

conditions (+AMB plots). Porewater salinity, pH, SO<sub>4</sub><sup>2-</sup>, NH<sub>4</sub><sup>+</sup>, and TDN increased with added 292 293 salinity, while porewater DOC decreased (P < 0.10; Table 2). There was no change in 294 temperature, alkalinity, SRP, and TDP with added salinity (P > 0.10; Fig. 2, Fig. 3). At the BW site, porewater salinity in the +SALT plots ranged from  $11.24 \pm 0.43$  to 19.37 ppt  $\pm 0.25$  (Fig. 295 296 2d). On average, porewater salinity was  $4.71 \pm 0.40$  ppt higher in the +SALT plots compared to 297 the +AMB plots. Porewater salinity and SO<sub>4</sub><sup>2</sup>- increased with added salinity, while alkalinity, 298 DOC, NH<sub>4</sub><sup>+</sup>, TDN, SRP, and TDP all decreased with added salinity (Table 2; P < 0.10). 299 Porewater SRP and TDP were 1-2 orders of magnitude higher at the BW site compared to the 300 FW site. 301 Porewater HS<sup>-</sup> was two orders of magnitude higher at the BW site compared to the FW 302 site (Fig. 4). At the FW site, porewater HS<sup>-</sup> was undetectable in the +AMB plots and elevated in 303 the +SALT plots (0.08  $\pm$  0.01 mM; P < 0.001). At the BW site, porewater HS<sup>-</sup> was lower in the 304 +SALT plots compared to the +AMB plots (1.20  $\pm$  0.12 vs. 2.88  $\pm$  0.12 mM; P < 0.001). There 305 was no difference in redox potential between the +AMB and +SALT plots at the FW site 306 (Appendix S1: Fig. S1; P = 0.252). At the BW site, redox potential was significantly higher in 307 the +SALT plots compared to the +AMB and "no-chamber" control plots (Appendix S1: Fig. S1; 308 P < 0.001). 309 Ambient porewater salinity at the BW site changed distinctly over the study period, 310 elevating from  $8.0 \pm 0.3$  ppt (Oct 2014) to  $12.0 \pm 0.4$  ppt (Oct 2016; Fig. 5). Distinct change-311 points were detected using a 3-way piecewise regression ( $r^2 = 0.943$ ,  $F_{(7.24)} = 40.46$ , P < 0.001) 312 and corresponded with periods where water receded below or rose above the soil surface (Fig. 5). 313 Mean salinity of each change-point can be found in Appendix S1: Table S1.

314

315

# Species Richness, Culm Density, and Above- and Below-ground Biomass

316 There was no difference in E. cellulosa stem density between the +AMB (185  $\pm$  23 plants 317 plot<sup>1</sup>) and +SALT (152  $\pm$  21 plants plot<sup>1</sup>) plots at the FW site (P > 0.10). Macrophyte species 318 richness at the FW site was not significantly different between the +AMB and +SALT treatments 319 during the first year  $(4.1 \pm 0.3 \text{ vs. } 4.3 \pm 0.2 \text{ species plot}^{-1}, \text{ respectively})$ ; however, +SALT plots 320 had fewer species per plot  $(2.9 \pm 0.2)$  compared to the +AMB treatment after the second year of 321 dosing  $(3.8 \pm 0.3; t = 3.77, P < 0.001)$ . 322 At the FW site, saltwater additions caused no change in sawgrass culm density or 323 aboveground biomass after two years (P > 0.10; Table 3; Fig. 6). At the BW site, there was a 324 delayed response. Sawgrass culm density in the +SALT plots did not significantly differentiate 325 from the +AMB plots until Oct 2016 (LSMEANS, t = 2.51, P = 0.030), two years after saltwater 326 additions began. Similarly, we found no significant differentiation in aboveground biomass in +SALT plots until Dec 2016 (LSMEANS, t = 2.27, P = 0.046; Fig. 6a). ANPP was depressed in 327 328 the second year at the BW site in the +SALT plots  $(307 \pm 101 \text{ gdw m}^2)$  compared to the +AMB 329 plots  $(504 \pm 146 \text{ gdw m}^{-2})$ , but this effect was not significant (P > 0.10; Fig. 7). There was no 330 change in ANPP with salt addition at the FW site (P > 0.10). Sawgrass culm density, 331 aboveground biomass, and ANPP were less at the FW site compared to the BW site. Sawgrass 332 leaf nutrient-level response to salt dosing varied by site (Table 4). At both sites, sawgrass C concentration did not change with saltwater addition (ANOVA, P > 0.10). At the BW site, both 333 334 sawgrass leaf N and P increased with added salinity after both 1 and 2 years (Table 4). Sawgrass 335 leaf N and P at the FW site were stable across treatments. 336 Two years after saltwater dosing was initiated, live belowground biomass at both sites 337 decreased. At the BW site, live root biomass declined at all depths with added salinity

 $(F_{(1,30)}=6.69, P=0.014)$ , but this result was only significant in the top 10-cm and when all three depths were combined (Tukey HSD, P < 0.10; Table 5). Results were similar at the FW site: live root biomass declined at all depths with added salinity  $(F_{(1,30)}=13.99, P<0.001)$ , and this result was only significant in the top 10-cm and when all three depths were combined (Tukey HSD, P < 0.10; Table 5). There was no significant difference in live root biomass at 0-10 and 10-20 cm depths when comparing the FW +AMB and the BW +AMB plots, but the BW site had less live root biomass compared to the FW site at the 20-30 cm depth horizon (t = 22.0, P = 0.004) and with all combined depths (t = 260.0, P = 0.022; Table 5).

#### Ecosystem Carbon Flux

There was no difference between the "no-chamber" control and the +AMB plots for any flux measurement and on any date (P > 0.10; Table 6). Therefore, we only compared the results between the +SALT and +AMB plots. Rates of ER<sub>CO2</sub> and NEP had seasonal patterns directly related to inundation at both sites (Fig. 8), with each site taking up CO<sub>2</sub> when inundated but releasing CO<sub>2</sub> when water receded below the soil surface. ER<sub>CO2</sub> was directly correlated with water level, maxing out at 6.7  $\mu$ mol CO<sub>2</sub> mr<sup>2</sup> s<sup>-1</sup> (BW, +SALT, Jul 2015) and 10.8  $\mu$ mol CO<sub>2</sub> mr<sup>2</sup> s<sup>-1</sup> (FW, +AMB, Apr 2015) at each site when soil was exposed (Fig. 8). Overall, ER<sub>CO2</sub> was greater (ANOVA, P < 0.10) when soil was exposed at each site (Table 6).

At the FW site, added salt caused a reduction in NEP, GEP, and ER<sub>CO2</sub> (P < 0.10; Table 3) when the site was inundated, though this result was strongly time-dependent and occurred only for three months following dry-down (Fig. 8). There were no effects of elevated salinity on NEP, GEP, and ER<sub>CO2</sub> when the site FW was dry (P > 0.10; Table 6). When soil at the FW site was exposed, added salt caused greater ER<sub>CH4</sub>; however, because of high variability and lack of

months in which the soil was exposed during drawdown, this result was not significant over the duration of the experiment (P > 0.10). Soil CO<sub>2</sub> efflux during May 2015 was higher in the +AMB plots compared to the +SALT plots ( $1.27 \pm 0.14$  vs.  $0.88 \pm 0.05$  µmol m<sup>-2</sup> s<sup>-1</sup>, respectively; t = 2.61, P = 0.029).

At the BW site, added salt had no effect on NEP, GEP, ER<sub>CO2</sub>, ER<sub>CH4</sub>, and soil CO<sub>2</sub> efflux (P > 0.10; Table 3) when the site was wet (Table 6). When soil at the BW site was exposed, there was no difference between treatments (P > 0.10) in GEP, ER<sub>CO2</sub>, and ER<sub>CH4</sub> flux, but added salt decreased NEP (more CO<sub>2</sub> released) compared to the "no-chamber" control and +AMB plots (P = 0.008; Table 6). Soil CO<sub>2</sub> efflux during May 2015 was lower in the +AMB plots compared to the +SALT plots ( $0.60 \pm 0.08$  vs.  $0.96 \pm 0.10$  µmol m<sup>-2</sup> s<sup>-1</sup>, respectively; t = 2.55, P = 0.031).

## Discussion

Salinity pulses significantly changed porewater biogeochemistry and the net soil C balance. Hydrology (i.e., seasonal dry-down) was an important factor that interacted with salinity pulses to influence NEP. Pulses of elevated salinity reduced NEP at the FW marsh following a dry-down event, while elevated salinity only changed ecosystem CO<sub>2</sub> flux from the BW marsh during dry-down conditions. The decline in live root biomass at both sites under conditions of elevated salinity reflected reduced organic matter inputs into the soil and/or increased turnover of live to dead roots. These results confirmed our hypotheses that pulses of water with elevated salinity would change biogeochemical cycling and decrease plant root production and NEP, although the effect was site-dependent. We also confirmed that C loss was amplified during dry-down conditions at the BW site. We found that, even under ambient conditions, the BW marsh

was a net CO<sub>2</sub> source to the atmosphere, a potential mechanism for the collapse of peat observed at the site. Here we provide some of the first evidence from non-tidal, coastal peat marshes of biogeochemical responses to simulated saltwater intrusion.

387

388

389

390

391

392

393

394

395

396

397

398

399

400

401

402

403

404

405

406

384

385

386

#### Biogeochemical Responses to Salinity Pulses

Porewater chemistry varied dramatically by site in response to saltwater additions. Elevated salinity increased porewater SO<sub>4</sub><sup>2</sup>- at both the FW and BW sites (Fig. 2) as the brine solution we applied to the marshes contained SO<sub>4</sub><sup>2</sup>-concentrations mimicking those found in seawater. However, we did not see a significant suppression in CH<sub>4</sub> efflux with added saltwater at either the FW or BW site, most likely because of the high variability among measurements and our inability to detect episodic ebullition flux at a monthly sampling frequency (Goodrich et al. 2011, Comas and Wright 2012, 2014). We expected CH<sub>4</sub> efflux to be much higher at the FW compared to the BW site based on higher salinity (Poffenbarger et al. 2011), but we saw little difference between the two sites (Table 6). High water levels during measured flux could have allowed CH<sub>4</sub> diffused from the soil into the overlying water column to be oxidized (Megonigal and Schlesinger 2002, Reddy and DeLaune 2008), and therefore, we may not have a true estimate of CH<sub>4</sub> production at our sites. Additionally, CH<sub>4</sub> efflux was likely not higher at the FW site because P-limitation could be influencing CH<sub>4</sub> production (Amador and Jones 1993). Because of the long hydroperiods at our sites, they were covered with water at the outset of our study, so we were not able to measure initial soil CO<sub>2</sub> efflux. Instead, soil CO<sub>2</sub> flux was measurable only when water receded below the soil surface (dry-down in Feb 2015; Fig. 8). During this time, with pulses of elevated salinity water, soil CO<sub>2</sub> efflux decreased at the FW site. This was most likely the result of microbial stress combined with more oxic conditions

407

408

409

410

411

412

413

414

415

416

417

418

419

420

421

422

423

424

425

426

427

428

suppressing sulfate reduction and stimulating aerobic metabolism to the point where elevated SO<sub>4</sub><sup>2</sup>- from saltwater addition would not stimulate sulfate reduction (Mitsch and Gosselink 2007, Weston et al. 2011). Conversely, elevated salinity stimulated soil CO<sub>2</sub> efflux at the BW site. This same result was seen briefly for a period of approximately one week in mesocosm experiments using soil harvested at the BW site when they were exposed to elevated salinity and dry-down conditions (Wilson 2018). Therefore, although pulses of elevated salinity coupled with dry-down may initially stimulate soil CO<sub>2</sub> efflux, this stimulatory effect may not persist.

Porewater NH<sub>4</sub><sup>+</sup> and TDN increased with added salinity at the FW site (Fig. 3), possibly as a result of cations from the saltwater mix replacing adsorbed cations such as NH<sub>4</sub><sup>+</sup> in soils (Gardner et al. 1991, Ardón et al. 2013). Contrary to expectation, porewater alkalinity, DOC, NH<sub>4</sub><sup>+</sup>, TDN, SRP, TDP, and HS<sup>-</sup> all decreased at the BW site with saltwater addition (Fig. 2, Fig. 3, Fig. 4). In our study, there is evidence to suggest that lower porewater nutrient concentrations in the +SALT plots at the BW site may be caused by saltwater cation replacement. Our brine dosing solution mimicked the ionic composition of seawater, which is high in cations and is known to displace other cations adsorbed to soils, such as NH<sub>4</sub><sup>+</sup> and dissolved inorganic P (Gardner et al. 1991, Seitzinger et al. 1991, Fourqurean et al. 1992, Price et al. 2006). These minerals, now bioavailable, could have been taken up by macrophytes or microbes and incorporated into their biomass. Higher sawgrass leaf N and P content at our +SALT plots as compared to the +AMB plots at the BW site corroborates this hypothesis (Table 4). Greater leaf nutrient content within the +SALT plots could have also been caused by microbial cell death and lysis from excess salt, which would release nutrients and organic molecules into the surrounding porewater (Gobler et al. 1997), which could then be taken up by the plants. This release could

provide a temporary subsidy for brackish marsh plants to survive despite their relatively high-salinity and high-stress environments. More studies are needed to confirm this mechanism.

431

432

433

434

435

436

437

438

439

440

441

442

443

444

445

446

447

448

449

450

451

429

430

#### Ecosystem Carbon Cycling

Hydrology has been shown to strongly regulate exchange of CO<sub>2</sub> between the land and atmosphere in wetlands (Hao et al. 2011, Jimenez et al. 2012, Malone et al. 2013, Malone et al. 2014). The marshes we studied exhibited patterns of CO<sub>2</sub> flux in response to dry-down similar to other long-hydroperiod Everglades marshes by acting as a net CO<sub>2</sub> sink when water covered the soil surface and a net CO<sub>2</sub> source when water fell below the soil surface (Jimenez et al. 2012, Schedlbauer et al. 2012, Malone et al. 2014). During periods in which water was covering the soil surface, ER<sub>CO2</sub> was low and maximum potential GEP was high at both sites, leading to net CO<sub>2</sub> uptake around solar noon (Fig. 8). However, during periods when water receded below the soil surface, ER<sub>CO2</sub> spiked, likely due to greater aerobic respiration stimulation as a result of higher soil oxidation (Mitsch and Gosselink 2007, Webster et al. 2013), and these marshes switched from CO<sub>2</sub> sinks to net CO<sub>2</sub> sources to the atmosphere. GEP at our marsh sites was not affected during drought. Malone et al. (2013) saw a similar response in GEP and ER<sub>CO2</sub> in a sawgrass marsh exposed to dry-down conditions. To control for the addition of water in our +SALT plots, we added the same volume of ambient salinity water to our +AMB plots and took measurements on "no-chamber" control plots in which no water was added. We saw no difference in any flux measurements between the +AMB and no-water-added control plots during either the wet or dry period (Table 6), meaning that the physical act of adding more water to the plot during dosing had no measurable effect. This was likely because the amount of ambient water we added to each plot (<200 L) was not enough to substantially raise water levels

452

453

454

455

456

457

458

459

460

461

462

463

464

465

466

467

468

469

470

471

472

473

and affect GEP by decreasing exposed leaf area (Schedlbauer et al. 2010, Jimenez et al. 2012), and because water was already covering the surface, additional water dosing would not decrease ER<sub>CO2</sub> (Neubauer 2013).

Elevated salinity in coastal wetlands has been shown to alter ecosystem CO<sub>2</sub> cycling between the marsh and the atmosphere (Neubauer 2013, Weston et al. 2014). When the marshes in our study were wet, there was no effect on CO<sub>2</sub> flux with the addition of salinity, but when water receded below the soil surface, added salinity reduced NEP at the BW site (Table 6). Although mean GEP fell and mean ER<sub>CO2</sub> rose during dry-down in the added salinity plots at the BW site, these rates were not significantly different from the +AMB plots. NEP, however, was significantly greater in a negative direction, indicating that added salinity caused more CO2 to be released to the atmosphere. The rise in ER<sub>CO2</sub> with added salinity can be partially attributed to an increase in soil CO<sub>2</sub> efflux (Crow and Wieder 2005). Although we only have one month of soil CO<sub>2</sub> efflux measurements (May 2015), efflux increased by  $0.35 \pm 0.09 \,\mu\text{mol}$  CO<sub>2</sub> m<sup>-2</sup> s<sup>-1</sup> with added salinity compared to the +AMB plots, while during the same month, ERCO2 increased by 0.51±0.31 umol CO<sub>2</sub> m<sup>-2</sup> s<sup>-1</sup> with added salinity (Fig. 8e). Weston et al. (2011) measured a similar increase in soil CO<sub>2</sub> efflux with added salinity [0.60 (control) vs 0.71 (+salt) µmol CO<sub>2</sub> m<sup>-2</sup> s<sup>-1</sup>] when tidal freshwater marsh soils were exposed to oxic conditions. In addition, we may be underestimating overall CO<sub>2</sub> efflux from the marsh because we did not directly measure rates of diffusive CO<sub>2</sub> flux into the overlying water column and transport downstream. There was a negative linear relationship between water level and surface water alkalinity at both sites (Appendix S1: Fig. S1), indicating that as water levels dropped, CO<sub>2</sub> diffusing from the soil was becoming more concentrated in the overlying surface water.

474

475

476

477

478

479

480

481

482

483

484

485

486

487

488

489

490

491

492

493

494

495

496

Gross ecosystem productivity at the BW site also declined with added saltwater when no surface water was present (Fig. 8d). This response was a physiological effect because there was no decrease in biomass during this period (Fig. 6). Sulfide toxicity is a common stressor for wetland plants experiencing saltwater intrusion (Lamers et al. 1998). Lower sulfide and higher redox conditions in the +SALT plots at the BW site suggest that the plants were likely responding to osmotic stress of salt exposure rather than sulfide toxicity (Fig. 4, Appendix S1: Fig. S1). During times of low water availability, salt can accumulate in soils because little water flushes through the marsh (Ardón et al. 2013, Weston et al. 2014). Saltwater addition raised porewater salinities to between 16 and 20 ppt during the period when water was continuously below the soil surface (~Feb to Aug 2015; Fig. 2). High salinity causes osmotic stress, which rapidly decreases stomatal conductance and inhibits photosynthesis (Munns and Tester 2008). Sawgrass has been shown to significantly decrease productivity with continuous exposure to 20 ppt salinity (Wilson et al. in press). Because of low water flushing, porewater salinity did not significantly decline between 1 and 5 days after saltwater addition during dry periods, meaning that salinity was maintained at or near levels known to lead to a reduction in NEP (Appendix S1: Fig. S3; Wilson et al. in press). At the FW site, saltwater addition significantly decreased both GEP and ER<sub>CO2</sub>, but only

At the FW site, saltwater addition significantly decreased both GEP and ER<sub>CO2</sub>, but only immediately following the dry-down event (Fig. 8a,b). This is a similar response to the decline in both GEP and ER that Neubauer (2013) found with saltwater additions to a tidal freshwater marsh and is expected, given that GEP and ER are tightly linked (Cannell and Thornley 2000). This response was likely triggered by dry-down and its legacy effects. Both GEP and ER were lower with added saltwater compared to the +AMB plots for 3 months post-dry-down, resulting in significantly less CO<sub>2</sub> uptake with added salt (Fig. 8a-c). As little work has been done to study

coupled saltwater intrusion and drought effects on coastal wetlands, it is hard to pinpoint the exact mechanisms behind this response, though it may be due to decreased GEP in periphytic mats (Mazzei et al. 2018). These months (Mar-Aug 2015) were the only time in which porewater salinity at the FW site rose above 4 ppt, potentially resulting in osmotic stress and inhibiting stomatal conductance (Fig. 2; Munns and Tester 2008). As water levels rose, the effectiveness of our saltwater dosing diminished and allowed the marsh to recover to pre-dry-down conditions.

503

504

505

506

507

508

509

510

511

512

513

514

515

516

517

518

519

502

497

498

499

500

501

#### Aboveground Biomass

The salinity tolerance of sawgrass-dominated marshes varies widely and is likely dependent on soil type, hydraulic conductivity, and cation exchange capacity. Sawgrass has been shown to be tolerant of annual salinities up to 16.4 ppt, but plants flushing with lower salinity water (<5 ppt) in order to maintain their productivity (Troxler et al. 2014). Some studies have shown that sawgrass productivity begins to decrease when exposed to salinities as low as 5 ppt (Macek and Rejmankova 2007), while others have shown that sawgrass does have some tolerance to salinity and that aboveground biomass and productivity do not significantly decrease until continuous exposure of 20 ppt salinity (Wilson et al. 2018). We expected to see a significant decline in sawgrass aboveground biomass with added salinity in the field as well. However, our results suggest that, aboveground, sawgrass is tolerant to frequent pulses of low-level salinity in freshwater marshes, as there was no decline in aboveground biomass and ANPP (Fig. 6). Given that porewater salinity at the FW site never rose above 5 ppt, we would not expect to see much, if any, decline in aboveground biomass based on previous studies (Macek and Rejmankova 2007). At brackish marshes, however, cumulative salt loading and hydrology appear to impact sawgrass aboveground biomass, GEP, and ANPP (Fig. 6, Fig. 8d). At our BW study site,

porewater salinity in the +SALT treatment was much higher than the FW site and neared 20 ppt during some months (Fig. 2). Because these were pulses of salinity applied monthly rather than continuously, porewater salinity trended downward towards ambient levels 5 days after saltwater was added (Appendix S1: Fig. S1). We did observe lower culm density and aboveground biomass with added salinity compared to the +AMB plots toward the end of the 2-year sampling period at the BW site (Fig. 6), and a non-significant decline in ANPP during the second year (Fig. 7), indicating that increased exposure through continued pulses of elevated salinity appear to be having a negative effect on sawgrass growth in these brackish conditions, though continued monitoring of increased salinity exposure is needed to confirm this.

## Peat Vulnerability to Saltwater Intrusion

In peat marshes that receive little to no sediment input, such as the coastal Everglades, root production and litter turnover are the primary drivers of vertical peat accretion (Nyman et al. 2006, McKee 2011, Baustian et al. 2012). We measured a reduction in live root biomass with added salinity at both sites (Table 5). Little is known about how salt stress reduces initiation of new seminal or lateral roots, although osmotic stress usually reduces cell expansion in root tips (Munns and Tester 2008). Macek and Rejmankova (2007) found that relatively low elevated salinity (4-5 ppt) also decreased sawgrass root biomass. Generally, our BW site had significantly less live root biomass compared to the FW site (Table 5). Given that ambient salinity at the BW site was ~8-12 ppt and that low levels of porewater salinity (<5 ppt) led to significantly less live root biomass at the FW site, this result was not surprising but has consequences for the future of peat stability. Peat is a matrix of mostly organic matter (typically >80%; Table 1) with high porosity (>85%; (Nyman et al. 1990, Craft et al. 1993, Mitsch and Gosselink 2007). A loss of

live roots, and thus the main input of organic matter, could lead to peat destabilization. Deegan et al. (2012) found that N-enrichment in New England salt marshes led to peat destabilization and creek bank erosion, as *Spartina alterniflora* root-to-shoot allocation declined. Saltwater intrusion as well has been directly related to increased peat decomposition and a decrease in C accumulation (Whittle and Gallego-Sala 2016). DeLaune et al. (1994) found that saltwater intrusion caused mass plant mortality in a Gulf of Mexico brackish marsh, eventually resulting in peat collapse and conversion of the marsh to open water; the authors attributed this mainly to the loss of the living root network. This loss of the live root network in the peat soil matrix may be one mechanism leading to peat collapse at the BW site, evidenced by live standing sawgrass "pedestals" in which up to 30 cm of the root matrix is above the current soil surface (Wilson et al. 2018).

Marshes should continue to accrete vertically if the amount of C entering the marsh is greater than the amount of C leaving (Nyman et al. 2006, Weston et al. 2014). In non-tidal, non-riverine wetlands that receive little to no external organic matter inputs, such as sediments, estimating NEP is a robust way to determine if a marsh is accumulating C, although modern-day flux measurements tend to overestimate long-term C storage (Ratcliffe et al. 2018). We took our instantaneous flux measurements, and, using previously established ecosystem productivity response curves and methods (*see Supplemental Methods*), we performed an exercise to model GEP, ER<sub>CO2</sub>, and NEP to annual flux values (Neubauer 2013, Wilson et al. 2015). We found that NEP at the FW marsh was near C neutral (Fig. 9), which is what has been found at a nearby marsh using an eddy flux tower (Malone et al. 2014). Conversely, we found that the BW site was a large source of C to the atmosphere, even under ambient conditions (Fig. 9). Although not significant, pulses of elevated salinity led to a slight reduction in NEP at the FW site. A decline

in live roots and organic matter input into the soil, coupled with a shift of the marsh from a net sink to a net source as it transitions from fresh to brackish, creates conditions that leave coastal marshes vulnerable to peat collapse.

569

570

571

572

573

574

575

576

577

578

579

580

581

582

583

584

585

586

587

588

566

567

568

#### Water Management Effects on Carbon Flux

Water management decisions can play a critical role in determining how much water enters Everglades National Park (ENP) (Light and Dineen 1994, Ross et al. 2003). Because continuous sheet flow through this system has been largely cut off, periods of seasonal dry-down during low-rainfall years have a strong potential for altering freshwater marsh C cycling (Malone et al. 2014). At the BW site, C loss from the soil was amplified with pulses of elevated salinity water. This result raises important questions regarding how seasonal dry-down influences salinity at brackish water marshes and how future saltwater intrusion could alter C cycling within these marshes. Extreme seasonal dry-down in coastal wetlands, most often a function of altered hydrology, water management, and drought, can (i) increase salinity by reducing flushing and causing salt ion accumulation, (ii) increase the upstream reach of brackish water, and (iii) increase the salinity of tidal water (Anderson and Lockaby 2012, Ardón et al. 2013). In most coastal wetlands, this high salinity pulse is seasonal and returns to ambient levels when flushed by upstream freshwater inputs (Ardón et al. 2013, Weston et al. 2014). However, in the Florida coastal Everglades, surface water flow has been highly modified and is much slower (mean ~1 cm s<sup>-1</sup>; Schaffranek 2004) than most surface-flow-dominated wetlands (Light and Dineen 1994). This has reduced porewater flushing (Troxler et al. in press), allowed groundwater upwelling of high salinity water (Price et al. 2006), and contributed to a groundwater salt wedge that continues to move inland in ENP (Saha et al. 2011). Our results suggest that seasonal dry-downs, where the

water table falls below the soil surface for an extended period of time, may strongly control the ecological response of Everglades coastal wetlands to continued salinization.

Salt can accumulate in soils during seasonal dry-down because little water flushes through the marsh (Ardón et al. 2013, Weston et al. 2014). During a period of low rainfall in early 2015, ambient porewater salinity at the BW site rose quickly in a 3-month period and maintained near constant higher salinity for the next year despite high rainfall that resulted in high water table levels and low surface water salinity (Fig. 5). This change-point directly coincided with a period when water dropped below the soil surface. Other change-points occurred every time water rose above or receded below the soil surface. Our results suggest that low rainfall and low freshwater delivery produce extended dry-down and deeper drainage depth that may represent a significant catalyst of change in this coastal Everglades peat marsh. While some predictions about how climate change will affect drought frequency are contradictory (Sheffield et al. 2012, Dai 2013), it is predicted that droughts will set in more quickly and become more intense (Trenberth et al. 2014). The Central Everglades Plan, a recently authorized CERP project, will deliver the first increment of increased flow to the coastal Everglades and could potentially mitigate the effects of drought by keeping coastal marshes inundated for longer periods. Without this restoration, periods of drought could further salinize these brackish marshes, cause more C to be released to the atmosphere (Fig. 9), and result in peat collapse and transformation of marsh into open water.

608

609

610

611

589

590

591

592

593

594

595

596

597

598

599

600

601

602

603

604

605

606

607

# Acknowledgements

Funding for research was supported by Florida Sea Grant R/C-S-56, including cooperative agreements with the South Florida Water Management District, the Everglades Foundation, and

612

613

614

615

616

617

618

619

620

621

622

623

624

625

626

627

628

629

630

631

632

633

Everglades National Park. Additional funding was provided through the National Science Foundation's Florida Coastal Everglades Long Term Ecological Research (FCE LTER) Program (DEB-1237517). We thank Shawn Abrahams, Michelle Blaha, Marbelys Garriga, Adam Hines, Rowan Johnson, Oliver Ljustina, Melinda Martinez, Fabiola Santamaria, Chris Sillivan, Frank Skiff, Emily Standen, Ryan Stolee, and Mary Grace Thibault for help in the field. Len Scinto graciously provided lab resources for methane flux analysis. Joshua Allen provided descriptive details on coastal groundwater discharge in the coastal Everglades. Len Scinto and Steve Oberbauer provided valuable feedback on early drafts of this manuscript. The authors acknowledge the Everglades Depth Estimation Network (EDEN) project and the US Geological Survey for providing the water level and elevation data for the purpose of this research. Benjamin Wilson was supported by a Florida International University (FIU) Teaching Assistantship, Florida Sea Grant, FCE LTER and FIU Dissertation Year Fellowship. Hu was supported by the China Postdoctoral Science Foundation (2018M630731) and the National Science Foundation of China (41601102). This is publication number ## of the Sea Level Solutions Center and ## of the Southeast Environmental Research Center in the Institute of Water and Environment at Florida International University. Literature cited Allan, R. P., and B. J. Soden. 2008. Atmospheric warming and the amplification of precipitation extremes. Science 321:1481-1484. Amador, J. A., and R. D. Jones. 1993. Nutrient limitations on microbial respiration in peat soils with different total phosphorus content. Soil Biology & Biochemistry 25:793-801.

634 Anderson, C. J., and B. G. Lockaby. 2012. Seasonal patterns of river connectivity and saltwater 635 intrusion in tidal freshwater forested wetlands. River Research and Applications 28:814-636 826. 637 Ardón, M., J. L. Morse, B. P. Colman, and E. S. Bernhardt. 2013. Drought-induced saltwater 638 incursion leads to increased wetland nitrogen export. Global Change Biology 19:2976-639 2985. 640 Atkinson, M. J., and C. Bingman. 1997. Elemental composition of commercial seasalts. Journal 641 of Aquariculture and Aquatic Sciences 3:39-43. 642 Baustian, J. J., I. A. Mendelssohn, and M. W. Hester. 2012. Vegetation's importance in 643 regulating surface elevation in a coastal salt marsh facing elevated rates of sea level rise. 644 Global Change Biology 18:3377-3382. 645 Burdige, D. J. 2006. Geochemistry of marine sediments. Princeton University Press, Princeton. 646 Cannell, M. G. R., and J. H. M. Thornley. 2000. Modelling the components of plant respiration: 647 Some guiding principles. Annals of Botany 85:45-54. 648 Capone, D. G., and R. P. Kiene. 1988. Comparison of microbial dynamics in marine and fresh 649 water sediments - contrasts in anaerobic carbon catabolism. Limnology and 650 Oceanography **33**:725-749. 651 Chambers, L. G., S. E. Davis, T. T. Troxler, J. N. Boyer, A. Downey-Wall, and L. J. Scinto. 652 2013. Biogeochemical effects of simulated sea level rise on carbon loss in an Everglades 653 mangrove peat soil. Hydrobiologia:doi 10.1007/s10750-10013-11764-10756. 654 Chambers, L. G., K. R. Reddy, and T. Z. Osborne. 2011. Short-Term Response of Carbon 655 Cycling to Salinity Pulses in a Freshwater Wetland. Soil Science Society of America 656 Journal 75:2000-2007.

657 Childers, D. L., D. Iwaniec, D. Rondeau, G. Rubio, E. Verdon, and C. J. Madden. 2006. 658 Responses of sawgrass and spikerush to variation in hydrologic drivers and salinity in 659 Southern Everglades marshes. Hydrobiologia **569**:273-292. 660 Chmura, G. L., S. C. Anisfeld, D. R. Cahoon, and J. C. Lynch. 2003. Global carbon sequestration 661 in tidal, saline wetland soils. Global Biogeochemical Cycles 17:12. 662 Comas, X., and W. Wright. 2012. Heterogeneity of biogenic gas ebullition in subtropical peat 663 soils is revealed using time-lapse cameras. Water Resources Research 48. 664 Comas, X., and W. Wright. 2014. Investigating carbon flux variability in subtropical peat soils of 665 the Everglades using hydrogeophysical methods. Journal of Geophysical Research-666 Biogeosciences 119:1506-1519. 667 Cormier, N., K. W. Krauss, and W. H. Conner. 2013. Periodicity in Stem Growth and Litterfall 668 in Tidal Freshwater Forested Wetlands: Influence of Salinity and Drought on Nitrogen 669 Recycling. Estuaries and Coasts 36:533-546. 670 Craft, C., J. Clough, J. Ehman, S. Joye, R. Park, S. Pennings, H. Guo, and M. Machmuller. 2009. 671 Forecasting the effects of accelerated sea-level rise on tidal marsh ecosystem services. 672 Frontiers in Ecology and the Environment 7:73-78. 673 Craft, C. B., E. D. Seneca, and S. W. Broome. 1993. Vertical accretion in microtidal regularly 674 and irregularly flooded estuarine marshes. Estuarine Coastal and Shelf Science 37:371-675 386. 676 Crow, S. E., and R. K. Wieder. 2005. Sources of Co-2 emission from a northern peatland: Root 677 respiration, exudation, and decomposition. Ecology 86:1825-1834. 678 Dai, A. G. 2013. Increasing drought under global warming in observations and models. Nature 679 Climate Change 3:52-58.

680 Daoust, R. J., and D. L. Childers. 1998. Quantifying aboveground biomass and estimating net 681 aboveground primary production for wetland macrophytes using a non-destructive 682 phenometric technique. Aquatic Botany 62:115-133. 683 Davis, S. M., L. H. Gunderson, W. A. Park, J. R. Richardson, and J. E. Matteson. 1994. 684 Landscape dimension, composition, and function in a changing Everglades ecosystem. 685 Pages 419-444 in S. M. Davis and J. C. Ogden, editors. Everglades: The Ecosystem and 686 its Restoration. St. Lucie Press, Delray Beach. 687 Deegan, L. A., D. S. Johnson, R. S. Warren, B. J. Peterson, J. W. Fleeger, S. Fagherazzi, and W. 688 M. Wollheim. 2012. Coastal eutrophication as a driver of salt marsh loss. Nature 689 **490**:388-+. 690 Delaune, R. D., J. A. Nyman, and W. H. Patrick. 1994. Peat collapse, ponding and wetland loss 691 in a rapidly submerging coastal marsh. Journal of Coastal Research 10:1021-1030. 692 Delaune, R. D., C. J. Smith, and W. H. Patrick. 1983. Methane release from gulf-coast wetlands. 693 Tellus Series B-Chemical and Physical Meteorology 35:8-15. 694 Duarte, C. M., J. J. Middelburg, and N. Caraco. 2005. Major role of marine vegetation on the 695 oceanic carbon cycle. Biogeosciences 2:1-8. 696 Faulkner, S. P., W. H. Patrick, and R. P. Gambrell. 1989. Field techniques for measuring wetland 697 soil parameters. Soil Science Society of America Journal 53:883-890. 698 Fourqurean, J. W., J. C. Zieman, and G. V. N. Powell. 1992. Relationships between porewater 699 nutrients and seagrasses in a subtropical carbonate environment. Marine Biology 114:57-700 65.

701 Gardner, W. S., S. P. Seitzinger, and J. M. Malczyk. 1991. The effects of sea salts on the forms 702 of nitrogen released from estuarine and fresh-water sediments - does ion-pairing affect 703 ammonium flux. Estuaries 14:157-166. 704 Giblin, A. E., N. B. Weston, G. T. Banta, J. Tucker, and C. S. Hopkinson. 2010. The Effects of 705 Salinity on Nitrogen Losses from an Oligohaline Estuarine Sediment. Estuaries and 706 Coasts 33:1054-1068. 707 Gobler, C. J., D. A. Hutchins, N. S. Fisher, E. M. Cosper, and S. A. Sanudo-Wilhelmy. 1997. 708 Release and bioavailability of C, N, P, Se, and Fe following viral lysis of a marine 709 chrysophyte. Limnology and Oceanography 42:1492-1504. 710 Goodrich, J. P. G. J. P., R. K. Varner, S. Frolking, B. N. Duncan, and P. M. Crill. 2011. Highfrequency measurements of methane ebullition over a growing season at a temperate 711 712 peatland site. Geophysical Research Letters 38:DOI: 10.1029/2011GL046915. 713 Hao, Y. B., X. Y. Cui, Y. F. Wang, X. R. Mei, X. M. Kang, N. Wu, P. Luo, and D. Zhu. 2011. 714 Predominance of Precipitation and Temperature Controls on Ecosystem CO2 Exchange 715 in Zoige Alpine Wetlands of Southwest China. Wetlands 31:413-422. 716 Herbert, E. R., P. Boon, A. J. Burgin, S. C. Neubauer, R. B. Franklin, M. Ardón, K. N. 717 Hopfensperger, L. P. M. Lamers, and P. Gell. 2015. A global perspective on wetland 718 salinization: ecological consequences of a growing threat to freshwater wetlands. 719 Ecosphere 6. 720 Herbert, E. R., J. Schubauer-Berigan, and C. B. Craft. 2018. Differential effects of chronic and 721 acute simulated seawater intrusion on tidal freshwater marsh carbon cycling. 722 Biogeochemistry 138:137-154.

723 Hohner, S. M., and T. W. Dreschel. 2015. Everglades peats: using historical and recent data to 724 estimate predrainage and current volumes, masses and carbon contents. Mires and Peat 725 **16**. 726 Jerath, M., M. Bhat, V. H. Rivera-Monroy, E. Castaneda-Moya, M. Simard, and R. R. Twilley. 727 2016. The role of economic, policy, and ecological factors in estimating the value of 728 carbon stocks in Everglades mangrove forests, South Florida, USA. Environmental 729 Science & Policy 66:160-169. 730 Jimenez, K. L., G. Starr, C. L. Staudhammer, J. L. Schedlbauer, H. W. Loescher, S. L. Malone, 731 and S. F. Oberbauer. 2012. Carbon dioxide exchange rates from short- and long-732 hydroperiod Everglades freshwater marsh. Journal of Geophysical Research-733 Biogeosciences 117. 734 Lamers, L. P. M., H. B. M. Tomassen, and J. G. M. Roelofs. 1998. Sulfate-induced 735 entrophication and phytotoxicity in freshwater wetlands. Environmental Science & 736 Technology **32**:199-205. 737 Lenth, R.V. 2017. Using Ismeans. https://cran.r-738 project.org/web/packages/lsmeans/vignettes/using-lsmeans.pdf 739 Li, L. F., W. H. Li, and Y. Kushnir. 2012. Variation of the North Atlantic subtropical high 740 western ridge and its implication to Southeastern US summer precipitation. Climate 741 Dynamics **39**:1401-1412. 742 Light, S. S., and J. W. Dineen. 1994. Water control in the Everglades: A historical perspective. 743 Pages 47-84 in S. M. Davis and J. C. Ogden, editors. Everglades: The Ecosystem and its 744 Restoration. St. Lucie Press, Delray Beach.

745 Macek, P., and E. Reimankova. 2007. Response of emergent macrophytes to experimental 746 nutrient and salinity additions. Functional Ecology 21:478-488. 747 Malone, S. L., G. Starr, C. L. Staudhammer, and M. G. Ryan, 2013. Effects of simulated drought 748 on the carbon balance of Everglades short-hydroperiod marsh. 749 Malone, S. L., C. L. Staudhammer, S. F. Oberbauer, P. Olivas, M. G. Ryan, J. L. Schedlbauer, H. 750 W. Loescher, and G. Starr. 2014. El Nino Southern Oscillation (ENSO) Enhances CO2 751 Exchange Rates in Freshwater Marsh Ecosystems in the Florida Everglades. Plos One 9. 752 Mazzei, V., E. E. Gaiser, J. S. Kominoski, B. J. Wilson, S. Servais, L. Bauman, S. E. Davis, S. 753 Kelly, F. H. Sklar, D. T. Rudnick, J. Stachelek, and T. G. Troxler. 2018. Functional and 754 Compositional Responses of Periphyton Mats to Simulated Saltwater Intrusion in the Southern Everglades. Estuaries and Coasts. 755 756 McKee, K. L. 2011. Biophysical controls on accretion and elevation change in Caribbean 757 mangrove ecosystems. Estuarine Coastal and Shelf Science 91:475-483. 758 McKee, K. L., I. A. Mendelssohn, and M. W. Hester. 1988. Reexamination of pore water sulfide 759 concentrations and redox potentials near the aerial roots of Rhizophora mangle and 760 Avicennia germinans. American Journal of Botany 75:1352-1359. 761 McLeod, E., G. L. Chmura, S. Bouillon, R. Salm, M. Bjork, C. M. Duarte, C. E. Lovelock, W. H. 762 Schlesinger, and B. R. Silliman. 2011. A blueprint for blue carbon: toward an improved 763 understanding of the role of vegetated coastal habitats in sequestering CO2. Frontiers in 764 Ecology and the Environment 9:552-560. 765 McVoy, C. W., W. P. Said, J. Obeysekera, J. Van Arman, and T. W. Dreschel. 2011. Landscapes 766 and Hydrology of the Predrainage Everglades. University of Florida Press, Gainesville, 767 FL.

788

768 Megonigal, J. P., and W. H. Schlesinger. 2002. Methane-limited methanotrophy in tidal 769 freshwater swamps. Global Biogeochemical Cycles 16. 770 Mitsch, W. J., and J. G. Gosselink. 2007. Wetlands. 4th ed. edition. John Wiley & Sons, Inc., 771 Hoboken, NJ. 772 Munns, R., and M. Tester. 2008. Mechanisms of salinity tolerance. Annual Review of Plant 773 Biology **59**:651-681. 774 National Academies of Sciences, E., and Medicine. 2016. Progress Toward Restoring the 775 Everglades: The Sixth Biennial Review - 2016. The National Academies Press, 776 Washington D.C. 777 Neubauer, S. C. 2013. Ecosystem responses of a tidal freshwater marsh experiencing saltwater 778 intrusion and altered hydrology. Estuaries and Coasts 36:491-507. 779 Neubauer, S. C., W. D. Miller, and I. C. Anderson. 2000. Carbon cycling in a tidal freshwater 780 marsh ecosystem: a carbon gas flux study. Marine Ecology-Progress Series 199:13-30. 781 Nyman, J. A., R. D. Delaune, and W. H. Patrick. 1990. Wetland soil formation in the rapidly 782 subsiding Mississippi River Deltaic Plain - mineral and organic-matter relationships. 783 Estuarine Coastal and Shelf Science 31:57-69. 784 Nyman, J. A., R. J. Walters, R. D. Delaune, and W. H. Patrick, Jr. 2006. Marsh vertical accretion 785 via vegetative growth. Estuarine Coastal and Shelf Science 69:370-380. 786 Obeysekera, J., J. Barnes, and M. Nungesser. 2015. Climate Sensitivity Runs and Regional 787 Hydrologic Modeling for Predicting the Response of the Greater Florida Everglades

Ecosystem to Climate Change. Environmental Management 55:749-762.

789 Pinheiro J., Bates D., DebRoy S., Sarkar D., and R Core Team. 2017. nlme: Linear and 790 Nonlinear Mixed Effects Models. R package version 3.1-131, https://CRAN.R-791 project.org/package=nlme. 792 Poffenbarger, H. J., B. A. Needelman, and J. P. Megonigal. 2011. Salinity influence on methane 793 emissions from tidal marshes. Wetlands 31:831-842. 794 Price, R. M., P. K. Swart, and J. W. Fourqurean. 2006. Coastal groundwater discharge - an 795 additional source of phosphorus for the oligotrophic wetlands of the Everglades. 796 Hydrobiologia **569**:23-36. 797 Ratcliffe, J., R. Andersen, R. Andersen, R. Newton, D. Campbell, D. Mauguoy, and R. Payne. 798 2018. Contemporary carbon fluxes do not reflect the long-term carbon balance for an 799 Atlantic blanket bog. The Holocene **28**:140-149. 800 Reddy, K. R., and R. D. DeLaune. 2008. Biogeochemistry of wetlands: science and applications. 801 CRC Press, Boca Raton. 802 Ross, M. S., D. L. Reed, J. P. Sah, P. L. Ruiz, and M. T. Lewin. 2003. Vegetation: environment 803 relationships and water management in Shark Slough, Everglades National Park. 804 Wetlands Ecology and Management 11:291-303. 805 Saha, A. K., S. Saha, J. Sadle, J. Jiang, M. S. Ross, R. M. Price, L. Sternberg, and K. S. 806 Wendelberger. 2011. Sea level rise and South Florida coastal forests. Climatic Change 807 **107**:81-108. 808 Schaffranek, R. W. 2004. Sheet-flow Velocities and Factors Affecting Sheet-flow Behavior of 809 Importance to Restoration of the Florida Everglades. U.S. Geological Survey.

810 Schedlbauer, J. L., J. W. Munyon, S. F. Oberbauer, E. E. Gaiser, and G. Starr. 2012. Controls on 811 Ecosystem Carbon Dioxide Exchange in Short- and Long-Hydroperiod Florida 812 Everglades Freshwater Marshes. Wetlands 32:801-812. 813 Schedlbauer, J. L., S. F. Oberbauer, G. Starr, and K. L. Jimenez. 2010. Seasonal differences in 814 the CO(2) exchange of a short-hydroperiod Florida Everglades marsh. Agricultural and 815 Forest Meteorology **150**:994-1006. 816 Seitzinger, S. P., W. S. Gardner, and A. K. Spratt. 1991. The effect of salinity on ammonium 817 sorption in aquatic sediments - Implications for benthic nutrient recycling. Estuaries 818 **14**:167-174. 819 Sheffield, J., E. F. Wood, and M. L. Roderick. 2012. Little change in global drought over the 820 past 60 years. Nature **491**:435-+. 821 Sklar, F. H., M. J. Chimney, S. Newman, P. McCormick, D. Gawlik, S. L. Miao, C. McVoy, W. 822 Said, J. Newman, C. Coronado, G. Crozier, M. Korvela, and K. Rutchey. 2005. The 823 ecological-societal underpinnings of Everglades restoration. Frontiers in Ecology and the 824 Environment **3**:161-169. 825 Solorzano, L., and J. H. Sharp. 1980. Determination of total dissolved phosphorus and particulate 826 phosphorus in natural-waters. Limnology and Oceanography 25:754-757. 827 Spalding, E. A., and M. W. Hester. 2007. Interactive effects of hydrology and salinity on 828 oligohaline plant species productivity: Implications of relative sea-level rise. Estuaries 829 and Coasts 30:214-225. 830 Stachelek, J., S. P. Kelly, F. H. Sklar, C. Coronado-Molina, and T. Troxler. 2018. In situ 831 simulation of sea-level rise impacts on coastal wetlands using a flow-through mesocosm 832 approach. Methods in Ecology and Evolution.

833 Trenberth, K. E., A. G. Dai, G. van der Schrier, P. D. Jones, J. Barichivich, K. R. Briffa, and J. 834 Sheffield. 2014. Global warming and changes in drought. Nature Climate Change 4:17-835 22. 836 Troxler, T. G., D. L. Childers, and C. J. Madden. 2014. Drivers of Decadal-Scale Change in 837 Southern Everglades Wetland Macrophyte Communities of the Coastal Ecotone. 838 Wetlands **34**:S81-S90. 839 Wanless, H. R., and B. M. Vlaswinkel. 2005. Coastal landscape and channel evolution affecting 840 critical habitats at Cape Sable, Everglades National Park, Florida. 841 Webster, K. L., J. W. McLaughlin, Y. Kim, M. S. Packalen, and C. S. Li. 2013. Modelling 842 carbon dynamics and response to environmental change along a boreal fen nutrient 843 gradient. Ecological Modelling 248:148-164. 844 Weston, N. B., R. E. Dixon, and S. B. Joye. 2006. Ramifications of increased salinity in tidal 845 freshwater sediments: Geochemistry and microbial pathways of organic matter 846 mineralization. Journal of Geophysical Research-Biogeosciences 847 **111**:doi: 10.1029/2005JG000071. 848 Weston, N. B., A. E. Giblin, G. T. Banta, C. S. Hopkinson, and J. Tucker. 2010. The Effects of 849 Varying Salinity on Ammonium Exchange in Estuarine Sediments of the Parker River, 850 Massachusetts. Estuaries and Coasts 33:985-1003. 851 Weston, N. B., S. C. Neubauer, D. J. Velinsky, and M. A. Vile. 2014. Net ecosystem carbon 852 exchange and the greenhouse gas balance of tidal marshes along an estuarine salinity 853 gradient. Biogeochemistry 120:163-189.

854	Weston, N. B., M. A. Vile, S. C. Neubauer, and D. J. Velinsky. 2011. Accelerated microbial
855	organic matter mineralization following salt-water intrusion into tidal freshwater marsh
856	soils. Biogeochemistry 102:135-151.
857	Whittle, A., and A. V. Gallego-Sala. 2016. Vulnerability of the peatland carbon sink to sea-level
858	rise. Scientific Reports 6.
859	Wilson, B. J., B. Mortazavi, and R. P. Kiene. 2015. Spatial and temporal variability in carbon
860	dioxide and methane exchange at three coastal marshes along a salinity gradient in a
861	northern Gulf of Mexico estuary. Biogeochemistry 123:329-347.
862	Wilson, B.J., S. Servais, S. P. Charles, S. E. Davis, E. E. Gaiser, J. S. Kominoski, J. H. Richards,
863	and T. G. Troxler. 2018. Declines in plant productivity drive carbon loss from brackish
864	coastal wetland mesocosms exposed to saltwater intrusion. Estuaries and Coasts. In Press
865	Wright, A. L., and K. R. Reddy. 2001. Heterotrophic microbial activity in northern Everglades
866	wetland soils. Soil Science Society of America Journal 65:1856-1864.
867	Zhang, K., J. Dittmar, M. Ross, and C. Bergh. 2011. Assessment of sea level rise impacts on
868	human population and real property in the Florida Keys. Climatic Change 107:129-146.
869	Zimmermann, C. F., and C. W. Keefe. 1997. Method 440.0. Determination of carbon and
870	nitrogen in sediments and particulates of estuarine/coastal waters using elemental
871	analysis. U.S. Environmental Protection Agency, National Exposure Research
872	Laboratory, Office of Research and Development, Cincinnati, Ohio.
873	
874	

**Tables**876 Table 1. Soil physicochemical properties (mean  $\pm$  SE, n = 6) by site and by depth.

Site	Depth	Treatment	Bulk	Organic	Total C	Total N	Total P (%)
	(cm)		Density (g cm <sup>-3</sup> )	matter (%)	(%)	(%)	,
Freshwater	0-10	+AMB	$0.08 \pm 0.03$	$83.2 \pm 4.6$	$40.6 \pm 2.7$	$3.29 \pm 0.18$	$0.052 \pm 0.007$
		+SALT	$0.11 \pm 0.02$	$71.3 \pm 4.4$	$35.2 \pm 2.9$	$3.29 \pm 0.18$	$0.057 \pm 0.006$
	10-20	+AMB	$0.18 \pm 0.06$	$70.2 \pm 9.5$	$34.6 \pm 5.5$	$2.80\pm0.27$	$0.039 \pm 0.008$
		+SALT	$0.18 \pm 0.04$	$67.9 \pm 7.9$	$31.0 \pm 4.4$	$3.00\pm0.23$	$0.052\pm0.008$
	20-30	+AMB	$0.17 \pm 0.03$	$63.2 \pm 11.7$	$31.1 \pm 5.5$	$2.51 \pm 0.34$	$0.040\pm0.010$
		+SALT	$0.22 \pm 0.04$	$55.7 \pm 9.4$	$25.9 \pm 6.1$	$2.55\pm0.50$	$0.042 \pm 0.010$
Brackish water	0-10	+AMB	$0.07\pm0.02$	$85.8 \pm 2.7$	$42.7 \pm 0.9$	$2.47 \pm 0.31$	$0.052 \pm 0.007$
,,,,,,,,,,,,,,,,,,,,,,,,,,,,,,,,,,,,,,,		+SALT	$0.07 \pm 0.02$	$84.6 \pm 2.8$	$43.1\pm1.0$	$2.17 \pm 0.25$	$0.044 \pm 0.011$
	10-20	+AMB	$0.11 \pm 0.02$	$84.5 \pm 2.2$	$43.1 \pm 1.1$	$2.35 \pm 0.24$	$0.039 \pm 0.008$
		+SALT	$0.11 \pm 0.02$	$84.6 \pm 2.5$	$42.9 \pm 2.1$	$1.92 \pm 0.28$	$0.033 \pm 0.004$
	20-30	+AMB	$0.11 \pm 0.04$	$83.2 \pm 1.7$	$42.6\pm0.8$	$2.10 \pm 0.22$	$0.031 \pm 0.005$
		+SALT	$0.12\pm0.05$	$83.0\pm3.5$	$42.1\pm1.6$	$1.99 \pm 0.21$	$0.029\pm0.005$

880

881

882

883

884

Table 2. Full statistical results from a linear mixed model for porewater constituents from the freshwater (FW) and brackish water (BW) sites given treatment (trt) and date.

Site		Temperature		Salinity		pН	Alkalinity		SO <sub>4</sub> <sup>2</sup> -		DOC
FW	Trt	F(1,10) = 2.58 P = 0.112	个	F(1,10) = 1048 P < 0.001	$\uparrow$	F(1,10) = 22.79 P < 0.001	F(1,10) = 2. P = 0.105	.65	$ \uparrow F(1,10) = 910  P < 0.001 $	$\downarrow$	F(1,10) = 5.72 P = 0.017
	Date	F(21,199) = 125.5 P < 0.001		F(21,213) = 7.46 P < 0.001		F(19,189) = 21.9 P < 0.001	F(19,189) = P < 0.001	= 16.3	F(19,190) = 5.96 P < 0.001		F(19,188) = 4.77 P < 0.001
	Trt* Date	F(21,199) = 2.58 P < 0.001		F(21,213) = 6.32 P < 0.001		F(19,189) = 2.16 P = 0.004	F(19,189) = P < 0.001	= 3.76	F(19,190) = 5.51 P < 0.001		F(19,188) = 1.03 P = 0.427
BW	Trt	F(1,10) = 2.75 P = 0.098	$\downarrow$	F(1,10) = 301.8 P < 0.001	$\downarrow$	F(1,10) = 17.16 P < 0.001	$ \downarrow F(1,10) = 14 \\ P < 0.001 $	42.8	$\uparrow$ $F(1,10) = 223.5$ $P < 0.001$	$\downarrow$	F(1,10) = 157.9 P < 0.001
	Date	F(23,239) = 81.68 P < 0.001		F(23,239) = 32.2 P < 0.001		F(22,226) = 19.6 P < 0.001	F(22,227) = P < 0.001	= 12.2	F(22,227) = 21.3 P < 0.001		F(22,228) = 10.7 P < 0.001
	Trt* Date	F(23,239) = 1.19 P = 0.248		F(23,239) = 7.02 P < 0.001		F(22,226) = 4.12 P < 0.001	F(22,227) = P = 0.011	= 1.88	F(22,227) = 4.15 P < 0.001		F(22,228) = 1.86 P = 0.012

Site		NH <sub>4</sub> <sup>+</sup>	TDN	SRP	TDP	Sulfide	Redox
FW	Trt	$rac{F(1,10) = 176.2}{}$	f(1,10) = 178.2	F(1,10) = 0.09	F(1,10) = 1.50	f(1,10) = 302.3	F(1,10) = 21.80
		P < 0.001	P < 0.001	P = 0.761	P = 0.221	P < 0.001	P < 0.001
	Date	F(19,189) = 6.99	F(19,189) = 7.23	F(20,206) = 21.54	F(20,206) = 9.59	F(11,117) = 16.65	F(1,222) = 244.0
		P < 0.001	P < 0.001	P < 0.001	P < 0.001	P < 0.001	P < 0.001
	Trt*	F(19,189) = 1.43	F(19,189) = 1.30	F(20,206) = 2.53	F(20,206) = 3.15	F(11,117) = 12.81	F(1,222) = 0.83
	Date	P = 0.116	P = 0.184	P < 0.001	P < 0.001	P < 0.001	P = 0.363
BW	Trt	F(1,10) = 229.9	$\downarrow F(1,10) = 265.0$	$\downarrow$ $F(1,10) = 94.83$	$\downarrow F(1,10) = 99.36$	$\downarrow F(1,10) = 217.5$	F(1,10) = 1.47
		<i>P</i> < 0.001	P < 0.001	P < 0.001	P < 0.001	P < 0.001	P = 0.252
	Date	F(22,228) = 11.03	F(22,228) = 7.68	F(23,236) = 10.02	F(23,239) = 11.43	F(14,149) = 45.94	F(1,165) = 87.04
		P < 0.001	P < 0.001	P < 0.001	P < 0.001	P < 0.001	P < 0.001
	Trt*	F(22,228) = 2.28	F(22,228) = 2.74	F(23,236) = 2.86	F(23,239) = 4.39	F(14,149) = 7.16	F(1,165) = 5.09
	Date	P = 0.001	P = 0.012	P < 0.001	P < 0.001	P < 0.001	P = 0.025

Interpreted results in bold. Data presented as F(numerator degrees of freedom, denominator degrees of freedom) = F value, P = P

value. The arrows indicate, if significant, in what direction elevated salinity altered the given parameter.

885 DOC dissolved organic carbon,  $NH_4^+$  ammonium, TDN total dissolved nitrogen,  $SO_4^{2-}$  sulfate, TDP total dissolved phosphorus, SRP

886 soluble reactive phosphorus

Table 3. Full statistical results from a linear mixed model for all biomass and flux measurements.

Site		Aboveground Biomass	Culm Density	ANPP	GEP wet	GEP dry-
Freshwater	Treatment	F(1,10) = 0.19 P = 0.664	F(1,9) = 0.39 P = 0.546	F(1,9) = 0.02 P = 0.867	F(1,10) = 3.66 P = 0.084	F(1,9) = 1.56 P = 0.242
	Date	F(13,130) = 5.03 P < 0.001	F(13,115) = 5.08 P < 0.001	F(12,106) = 3.39 P < 0.001	F(14,134) = 5.58 P < 0.001	F(1,7) = 0.01 P = 0.899
	Treatment*	F(13,130) = 0.79	F(13,115) = 0.88	F(12,106) = 0.90	F(14,134) = 2.21	F(1,7) = 0.19
	Date	P=0.661	P = 0.570	P = 0.544	P = 0.010	P = 0.674
Brackish water	Treatment	F(1,10) = 1.30 P = 0.279	F(1,10) = 3.12 P = 0.107	F(1,10) = 0.74 P = 0.407	F(1,10) = 0.19 P = 0.671	F(1,10) = 1.28 P = 0.284
	Date	F(14,136) = 6.69	F(14,136) = 4.63	F(13,124) = 3.77	F(15,149) = 5.43	F(4,40) = 2.57
		P < 0.001	P < 0.001	P < 0.001	P < 0.001	P = 0.052
	Treatment* Date	F(14,136) = 1.29 P = 0.219	F(14,136) = 2.29 P = 0.007	F(13,124) = 1.39 P = 0.170	F(15,149) = 1.37 P = 0.165	F(4,40) = 1.56 P = 0.202

Site		ER <sub>CO2</sub> wet	ER <sub>CO2</sub> dry	NEP wet	NEP dry	CH <sub>4</sub> wet	CH <sub>4</sub> dry
Freshwater	Treatment	F(1,10) = 3.89	F(1,9) = 2.40	F(1,10) = 3.42	F(1,9) = 0.00	F(1,6) = 3.34	F(1,6) = 3.19
		P = 0.076	P = 0.155	P = 0.093	P = 0.953	P = 0.117	P = 0.124
	Date	F(14,134) = 8.32	F(1,7) = 14.30	F(14,135) = 4.96	F(1,8) = 6.73	F(1,44) = 3.14	F(1,4) = 3.63
		P < 0.001	P = 0.006	P < 0.001	P = 0.031	P = 0.083	P = 0.129
	Treatment*	F(14,134) = 1.45	F(1,7) = 5.54	F(14,135) = 1.98	F(1,8) = 1.08	F(1,44) = 7.88	F(1,4) = 3.96
	Date	P = 0.137	P = 0.057	P = 0.023	P = 0.327	P = 0.007	P = 0.117
Brackish water	Treatment	F(1,10) = 0.30 P = 0.594	F(1,10) = 2.43 P = 0.149	F(1,10) = 0.15 P = 0.699	F(1,10) = 210.89 P = 0.008	F(1,6) = 6.30 P = 0.045	F(1,6) = 5.05 P = 0.065
	Date	F(15,148) = 14.47	F(4,40) = 23.16	F(16,157) = 8.79	F(4,40) = 15.12	F(1,52) = 0.52	F(1,14) = 0.69
		P < 0.001	P < 0.001	P < 0.001	P < 0.001	P = 0.471	P = 0.419
	Treatment*	F(15,148) = 0.57	F(4,40) = 0.78	F(16,157) = 1.01	F(4,40) = 1.27	F(1,52) = 2.85	F(1,14) = 3.05
	Date	P = 0.887	P = 0.541	P = 0.446	P = 0.297	P = 0.097	P = 0.102

Interpreted results in bold. Data presented as F(numerator degrees of freedom, denominator degrees of freedom) = F value, P = P

890 value

889

- 891 ANPP aboveground net primary productivity, GEP gross ecosystem productivity, ERCO2 ecosystem respiration of carbon dioxide, NEP
- net ecosystem productivity, *CH*<sub>4</sub> methane.

Table 4. Mean  $(n=6) \pm SE$  of C, N, and P sawgrass leaf content for each year.

Site	Time	Treatment	C (mg g <sup>-1</sup> )	N (mg g <sup>-1</sup> )	P (μg g <sup>-1</sup> )	C:N:P
BW	Year 1	+AMB	$457\pm2.3^{\rm a}$	$9.09\pm0.25^{bc}$	$244\pm17^{ab}$	1872:37:1
		+SALT	$455\pm2.1^a$	$10.17\pm0.26^c$	$305\pm10^{c}$	1865:42:1
	Year 2	+AMB	$488 \pm 4.9^{b}$	$7.34 \pm 0.38^a$	$206\pm10^a$	2000:30:1
		+SALT	$480 \pm 1.6^{b}$	$8.55\pm0.42^{ab}$	$264 \pm 16^{bc}$	1967:35:1
FW	Year 1	+AMB	$456 \pm 3.7^a$	$7.74\pm0.19^{a}$	$232\pm13^a$	1869:32:1
		+SALT	$451 \pm 4.1^a$	$7.73\pm0.76^a$	$225\pm35^a$	1848:32:1
	Year 2	+AMB	NA	NA	NA	
		+SALT	NA	NA	NA	

Superscripted letters represent differences between year and treatment within a site from a two-

way ANOVA.

894

895

Table 5. Belowground live root biomass (mean  $\pm$  SE g C m<sup>-3</sup>) after two years of control (+AMB) and elevated salinity (+SALT) from each site, each treatment and from specific depths.

Site	Treatment	0-10	10-20	20-30	Total
BW	+AMB +SALT	$96 \pm 35^a$ $24 \pm 8^b$	$50\pm25^{ab}$ $12\pm3^{b}$	$14 \pm 4^b$ $9 \pm 2^b$	$159 \pm 43^{a}$ $45 \pm 9^{b}$
FW	+AMB +SALT	$87 \pm 24^a$ $19 \pm 6^b$	$79 \pm 12^{ab}$ $45 \pm 13^{ab}$	$76\pm29^{ab} \\ 21\pm3^{b}$	

A two-way ANOVA was run separately for each site with Treatment and Depth as factors. Total depth was compared for each site separately using an independent t-test. Different superscripts indicate a significant difference (P < 0.10).

Table 6. Mean  $\pm$  SE of net ecosystem productivity (NEP), gross ecosystem productivity (GEP), ecosystem respiration of CO<sub>2</sub> (ER<sub>CO2</sub>), and ecosystem respiration of CH<sub>4</sub> (ER<sub>CH4</sub>) from the brackish water (BW) and freshwater (FW) sites, separated by the "no-chamber" control, addition of ambient water (+AMB), and the addition of saltwater (+SALT) plots.

		CO <sub>2</sub> and CH <sub>4</sub> flux (µmol m <sup>-2</sup> s <sup>-1</sup> )						
		W	et	Dry				
Flux	<b>Treatment</b>	FW	$\mathbf{BW}$	FW	$\mathbf{BW}$			
NEP	Control	$3.23\pm0.44^a$	$3.06 \pm 0.47$	$-3.06 \pm 3.43$	$-1.25 \pm 0.61^{a}$			
	+AMB	$3.05\pm0.28^a$	$2.88 \pm 0.35$	$-2.24 \pm 2.86$	$\text{-}0.37 \pm 0.65^{a}$			
	+SALT	$2.38\pm0.16^b$	$2.52 \pm 0.27$	$-1.83 \pm 1.27$	$-2.44 \pm 0.90^{b}$			
GEP	Control	$4.41\pm0.51^a$	$5.54 \pm 0.49$	$5.95 \pm 1.49$	$2.61 \pm 0.42$			
	+AMB	$4.04\pm0.32^a$	$4.85 \pm 0.36$	$4.98 \pm 0.28$	$3.51 \pm 0.30$			
	+SALT	$3.08\pm0.20^b$	$4.20\pm0.21$	$3.23\pm0.32$	$2.51 \pm 0.41$			
ER <sub>CO2</sub>	Control	$1.18\pm0.09^{a}$	$2.65 \pm 0.26$	$9.01 \pm 4.92$	$3.87\pm0.57$			
	+AMB	$1.04\pm0.09^a$	$2.09 \pm 0.18$	$7.45 \pm 3.36$	$3.89 \pm 0.73$			
	+SALT	$0.75\pm0.06^{b}$	$1.77 \pm 0.15$	$5.05 \pm 0.95$	$4.95 \pm 0.78$			
ER <sub>CH4</sub>	Control	$0.110 \pm 0.043$	$0.043 \pm 0.023^a$	$0.009 \pm 0.019$	$-0.042 \pm 0.026$			
	+AMB	$0.121 \pm 0.036$	$0.026\pm0.011^a$	$-0.026 \pm 0.021$	$-0.039 \pm 0.015$			
	+SALT	$0.065 \pm 0.028$	$-0.005 \pm 0.017^{b}$	$0.108 \pm 0.142$	$0.027 \pm 0.053$			

Fluxes were separated into wet (water covering the soil surface) and dry (no surface water)

periods. A negative NEP indicates a flux from the marsh to the atmosphere. Superscripts represent the results of a two-way repeated measures ANOVA. Values without superscripts indicate that there was no significant difference between treatments for that parameter

913

914

915

916

917

918

919

920

921

922

923

924

925

926

927

928

929

930

931

932

933

934

935

**Figures** Figure 1. Experimental setup at the FW site (not to scale). The setup was similar at the BW site. Sixteen plots were established along a boardwalk, with a 3-m buffer zone between the saltwater amended plots and the ambient-water amended plots. "No-chamber" controls received no water additions. The +SALT plots were positioned downstream to minimize contamination of the control plots. Figure 2. Mean  $(n=6) \pm 1$  SE of monthly porewater temperature, salinity, pH, alkalinity, and sulfate (SO<sub>4</sub><sup>2</sup>-) from the freshwater (FW) and brackish water (BW) sites over the two-year duration of the study; samples taken at 15-cm depth from the ambient water (+AMB) and saltwater (+SALT) addition plots. Salinity is reported as parts per thousand, alkalinity, and SO<sub>4</sub><sup>2</sup>are reported in mg L<sup>-1</sup>. Figure 3. Mean (n=6) ± 1 SE of monthly porewater dissolved organic carbon (DOC), ammonium (NH<sub>4</sub><sup>+</sup>), total dissolved nitrogen (TDN), soluble reactive phosphorus (SRP), and total dissolved phosphorus (TDP) from the freshwater (FW) and brackish water (BW) sites over the two-year duration of the study; samples taken at 15-cm depth from the ambient water (+AMB) and saltwater (+SALT) addition plots. DOC, NH<sub>4</sub><sup>+</sup>, and TDN are reported in mg L<sup>-1</sup>, and SRP and TDP are reported in  $\mu g L^{-1}$ . Figure 4. Mean  $(n=6) \pm 1$  SE of monthly porewater sulfide at 15-cm depth at the freshwater (FW) and brackish water (BW) sites from the ambient-water amended (+AMB) and saltwater amended (+SALT) plots.

936 937 Figure 5. Mean  $(n=6) \pm 1$  SE of monthly porewater (PW) and surface water (SW) salinity and 938 939 940 941 942 943 944 945

daily water depth from the brackish water site within the +ambient-water plots. Soil surface is plotted as the 0-cm water mark (dashed line) to show its relation to water depth. Solid lines show

the results of a piecewise regression with relevant change-points for PW salinity

Figure 6. Change in *Cladium jamaicense* (sawgrass) culm density and aboveground live biomass over time at the freshwater (FW) and brackish water (BW) sites for the ambient-water amended (+AMB) and saltwater amended (+SALT) treatments. Points represent the monthly mean  $(n=6) \pm$ 1 SE. Stars above the data point indicate that there was a significant (LSMEANS, P < 0.10) difference among treatments for that site.

947

948

949

950

946

Figure 7. Annual mean  $(n=6) \pm 1$  SE of sawgrass aboveground net primary productivity (ANPP) separated by freshwater (FW) and brackish water (BW) site, ambient-water amended (+AMB) and saltwater amended (+SALT) treatments, and year.

951

952

953

954

955

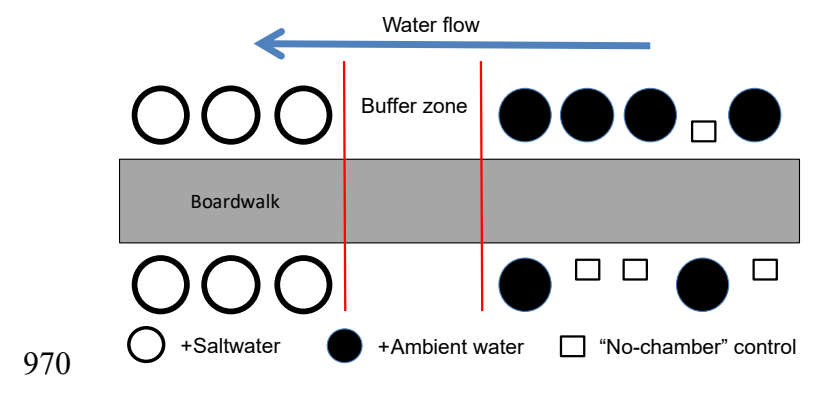
956

957

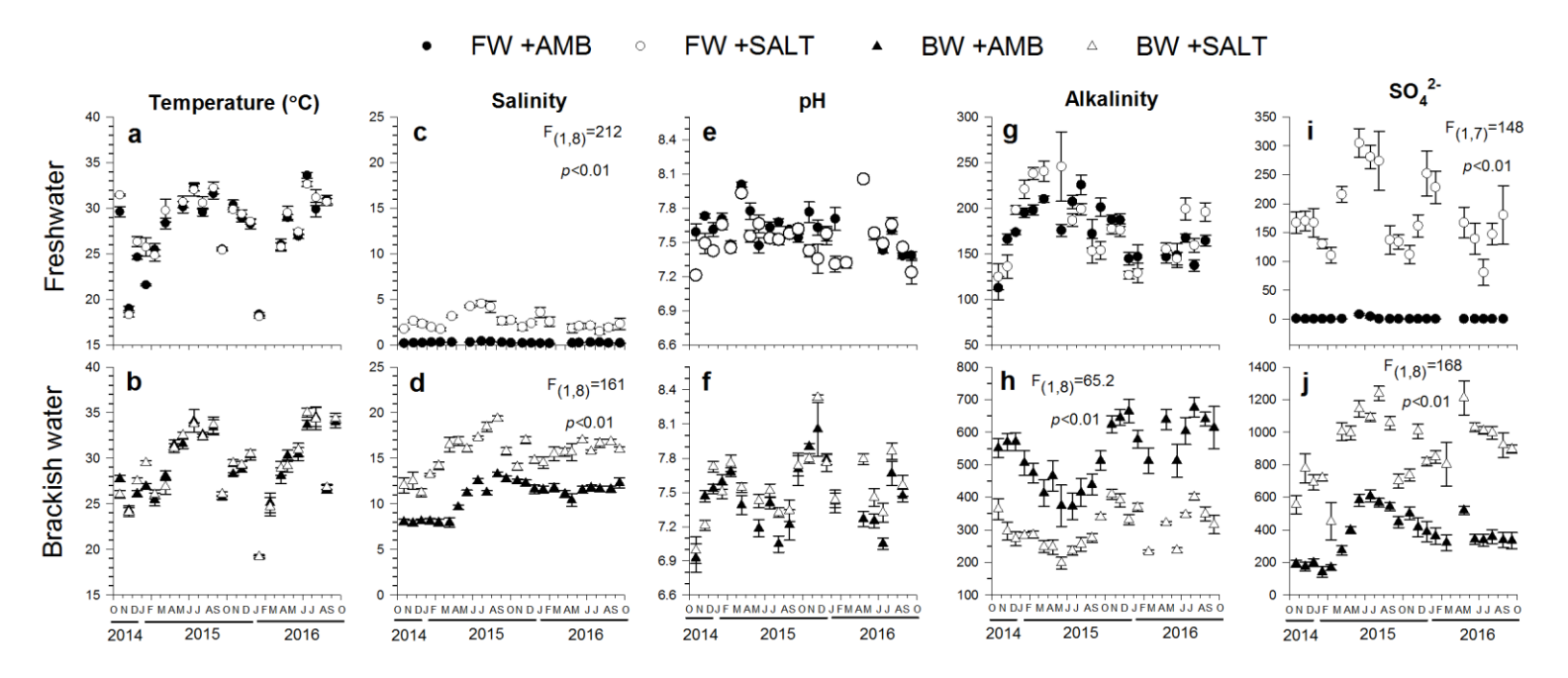
958

Figure 8. Instantaneous rates (mean,  $n=4\pm1$  SE) of freshwater gross ecosystem productivity (a; GEP), ecosystem respiration of CO<sub>2</sub> (b; ER), and net ecosystem productivity (c; NEP) and brackish water GEP (d), ERco2 (e), and NEP (f) over 2 years from both the freshwater and brackish water sites. The bottom panel also plots water level (blue line) in relation to the soil surface over time. For visual clarity, the "no-chamber" control plots were not added, as they were not significantly different from the +AMB plots (P > 0.10). Stars represent months in which treatments were significantly different from each other (LSMEANS, P < 0.10).

Figure 9. Estimated ecosystem C cycling over the two-year study period for net ecosystem productivity (NEP), gross ecosystem productivity (GEP), and ecosystem respiration of  $CO_2$  (ER $_{CO2}$ ) from the freshwater (FW) and brackish water (BW) sites and how it changes ambient water (+AMB) or saltwater (+SALT) pulses. A negative NEP indicates that the marsh is a net C source to the atmosphere. Values represent mean (n = 6)  $\pm 1$  SD flux over the experimental timeframe in g C m $^2$  y $^1$ . Annual flux was calculated using previously published GEP, PAR, ER, and temperature relationships for sawgrass (see Supplemental Methods) and previously derived light response curves for a sawgrass freshwater and brackish water marsh (Neubauer 2013, Wilson et al. 2015).

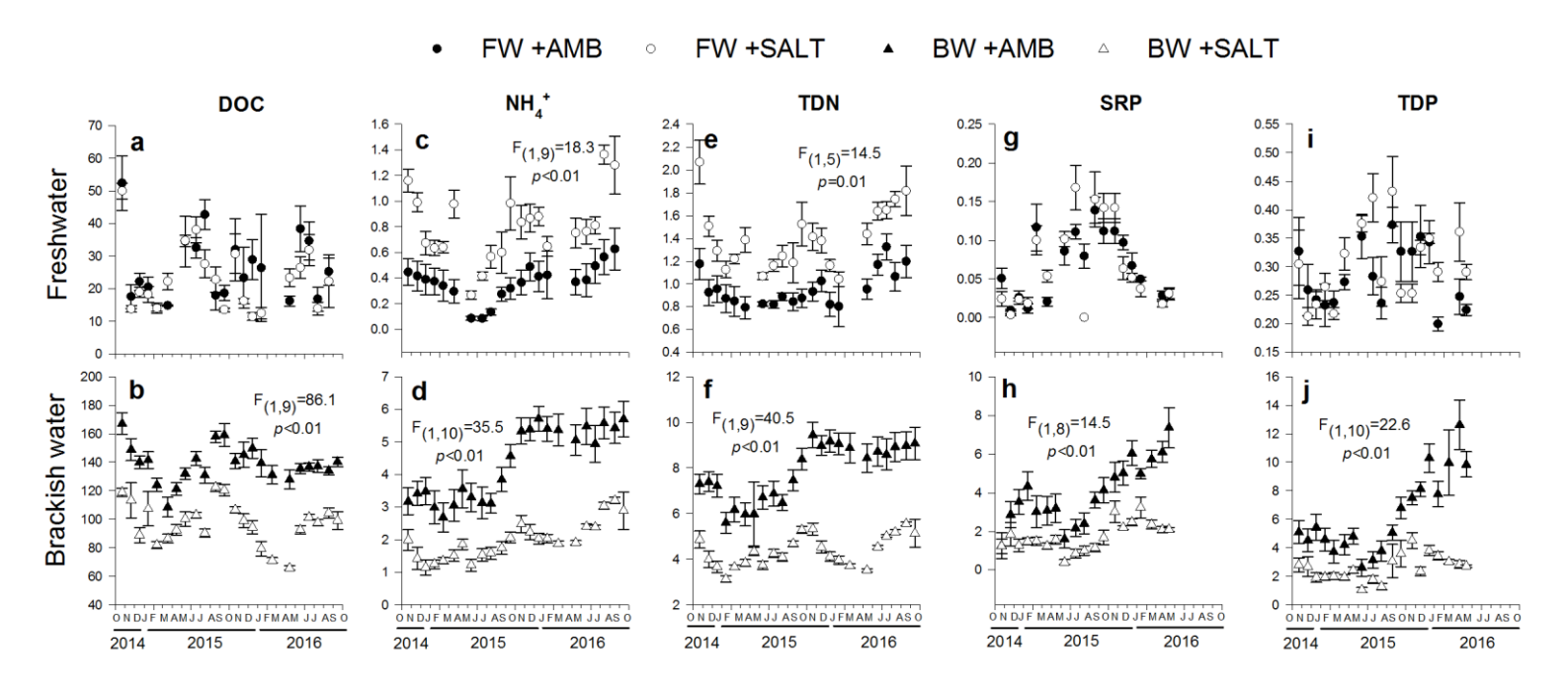


971 Figure 1.

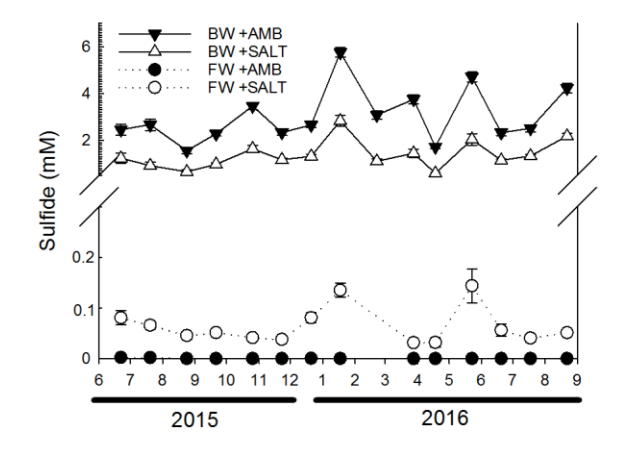


973 Figure 2.

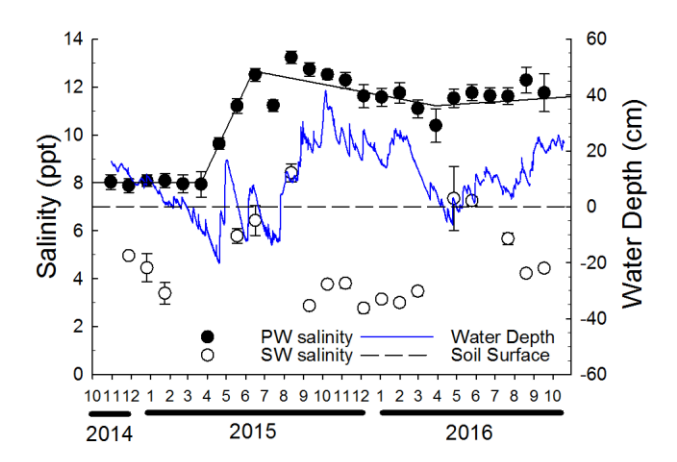
972



976 Figure 3.

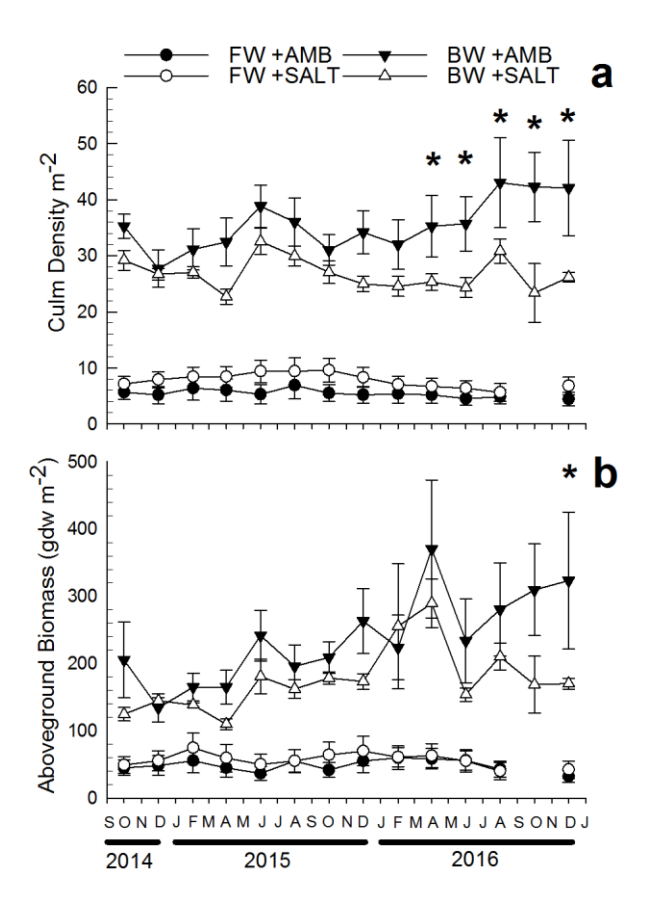


978 Figure 4.



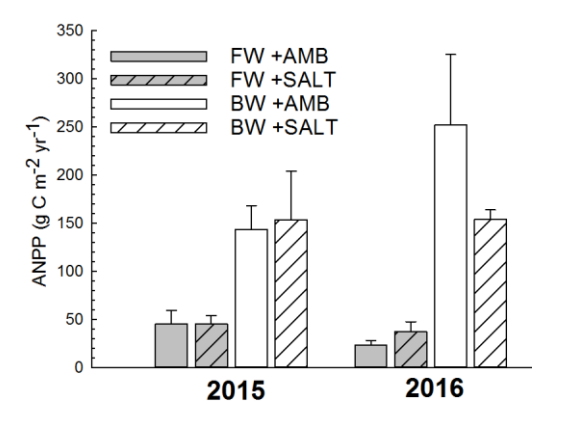
980 Figure 5.

981



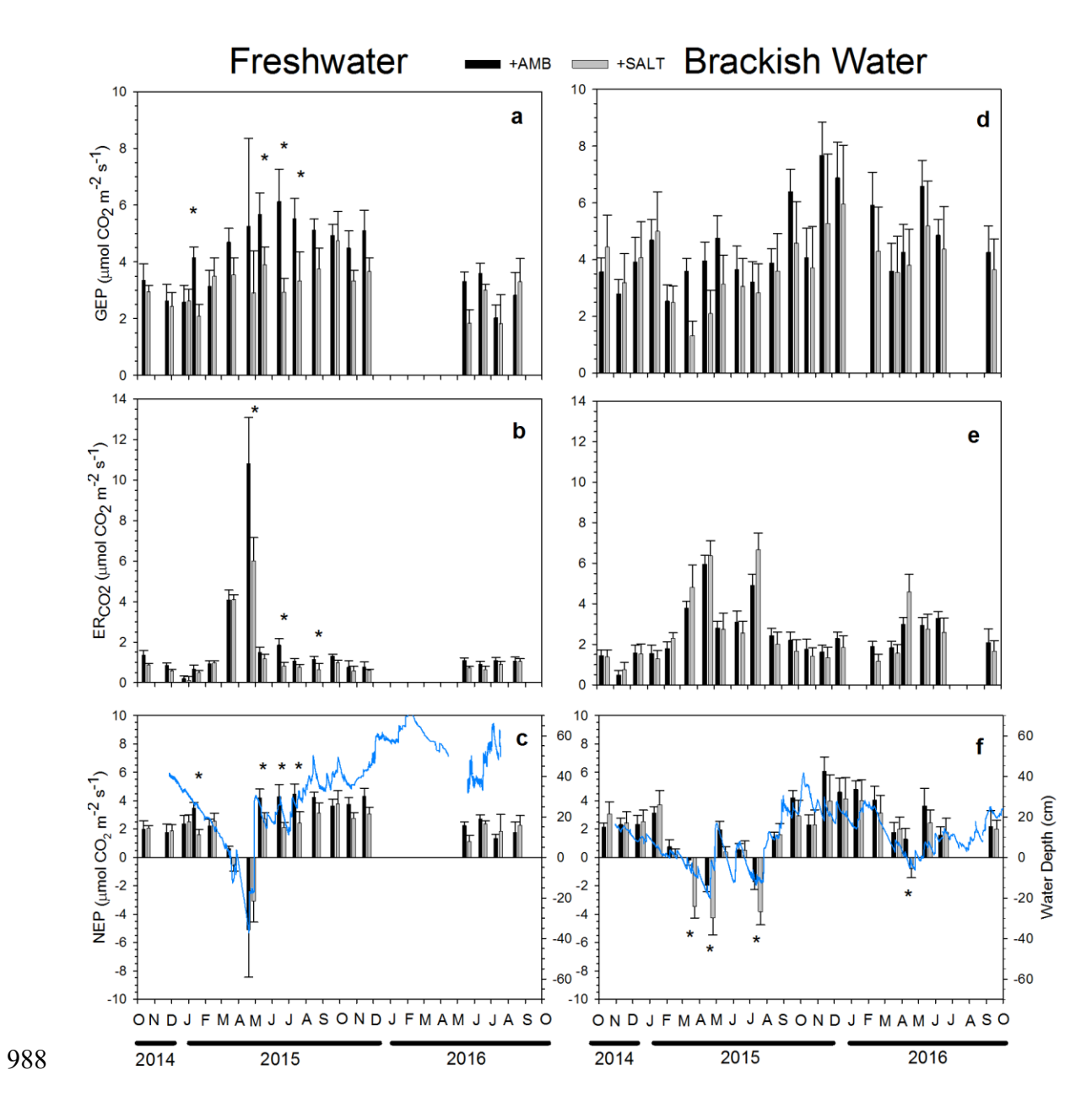
983 Figure 6.

982

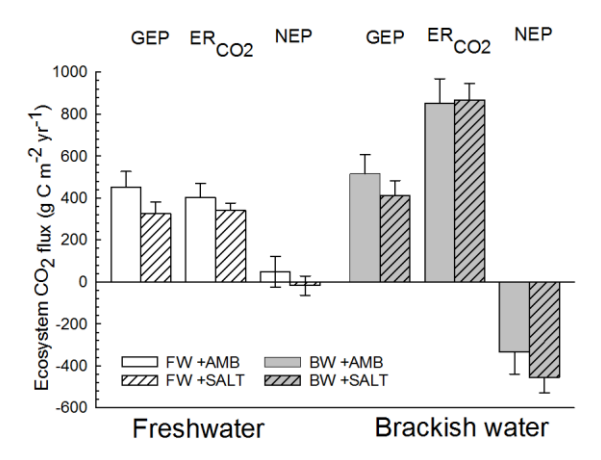


986 Figure 7.

987



989 Figure 8.



991 Figure 9.